University of Nevada, Reno

“Focused geologic mapping and structural analysis of the southern Eureka mining district; assessing structural controls and spatial patterns of mineralization”

A thesis submitted in partial fulfillment of the requirements for the degree of Master of Science in Geology

By

Russell Vincent Di Fiori

Sean Long, PhD, Advisor

May, 2014

THE GRADUATE SCHOOL

We recommend that the thesis
prepared under our supervision by

RUSSELL V. DI FIORI

Entitled

"Focused Geologic Mapping And Structural Analysis Of The Southern Eureka Mining District; Assessing Structural Controls And Spatial Patterns Of Mineralization"

be accepted in partial fulfillment of the
requirements for the degree of

MASTER OF SCIENCE

Sean P. Long, Phd, Advisor

John Muntean, Phd, Committee Member

William Hammond, Phd, Graduate School Representative

David W. Zeh, Ph.D., Dean, Graduate School

May, 2014

Abstract

The Eureka Mining District is located in the northern part of the Fish Creek Range in east-central Nevada. In this study, 1:6,000-scale geologic mapping and structural analysis were performed in the southern part of the district in order to identify structural controls on mineralization. This project bridges a gap between recent regional-scale mapping studies and detailed (<1:500) mapping performed in an active gold exploration campaign. A geologic map of a ~3.5 km (east-west) by ~8 km (north-south) region was generated, along with five deformed and restored cross-sections that illustrate the post- and pre-extensional deformation geometry. The stratigraphy of the map area consists of ca. 4 km of Cambrian to Devonian rocks that are dominated by carbonates, which, in turn, are unconformably overlain and intruded by Late Eocene silicic volcanic rocks.

The map area is composed of four distinct structural systems, including Early Cretaceous contractional structures which include the Eureka culmination and blind Ratto Canyon thrust, and three separate sets of normal faults: 1) 1st-order, km-scale offset, down-to-the-west normal faults, which include the Lookout Mountain and Dugout Tunnel faults, 2) 2nd-order, 10's to 100's meter-offset normal faults, including the Rocky Canyon, Oswego, and East Ratto Ridge fault systems, and 3) a 3rd-order set of sub-meter scale offset, east-striking extensional faults that offset the presumed Late Eocene jasperoid bodies. The 1st- and 2nd-order faulting can be bracketed between Late Cretaceous (ca. 86 Ma), the age of contact metamorphism in northern Rocky Canyon that is cut by the Dugout Tunnel fault, and Late Eocene (ca. 37 Ma), based on the overlapping relationship of a sub-volcanic unconformity.

The Eureka district is characterized by silver-lead polymetallic carbonate replacement and Carlin-type gold deposits, which are the two primary deposit-types in the project area. In addition to lithology and structure, specific types of hydrothermal alteration and mineralization were mapped, including

silicification, decarbonatization, dolomitization, quartz/calcite-veining, argillization, and the introduction of sulfides and their limonite weathering products. Through this method two distinct mineralization events were identified. Polymetallic mineralization, characterized by dolomitization, argillization, and quartz-veining, resides in the northern part of the map area in Rocky Canyon. It is interpreted to be genetically-related to Late Cretaceous granitic magmatism, which indicates that it pre-dates timing extension along 1st- and 2nd-order normal faults. The Carlin-type mineralization occurs as a series of deposits, mainly along Ratto Ridge. The deposits are associated with strong decarbonatization, strong silicification and jasperoid formation, and argillization. This Carlin-type deposit is temporally constrained to be pre- or syn-Late Eocene, due to overlap and intrusion of dated silicic-volcanic rocks.

The map area contains a kilometer-scale, synthetically-faulted relay-ramp of 2nd-order faults that transfer slip between the 1st-order, synthetic Dugout Tunnel and Lookout Mountain faults. Within accommodation zones, wall-damage zones are predicted to exert a first-order control on hydrothermal fluid pathways and localization of mineralization. The footwall of the Lookout Mountain fault contains a set of antithetic, 2nd-order normal faults, the East Ratto Ridge fault system, which is interpreted as a wall-damage zone that was fundamentally responsible for controlling fluid-flow that led to Carlin-type mineralization.

Acknowledgements

Foremost I thank my advisor, Dr. Sean Long, whom with infinite patience, constructive criticism, and unparalleled passion for ‘bigger-picture geology’, has taught me to distinguish the ‘forest from the trees’. I also thank Dr. John Muntean for his guidance and assistance with my thesis, and reiterating complex theories and processes in a simplified manner in a way my mind could comprehend. Thank you Gary Edmondo for your facilitation of this project and taking a chance on a naïve geologist that really just wanted to map rocks. The entire NBMG cartography team, especially Jennifer Mauldin, whom, without her I would still be lost somewhere in ArcMAP, pulling my hair out. I would also like to thank Dr. Bill Hammond for coming to the rescue and taking the third committee member seat on such short notice. I wish to thank Timberline Resources for their aid in funding and allowing me to utilize their property for such an awesome and rewarding project. A big thank you goes out to my fellow graduate students at UNR. Specifically, Ryan Anderson, Greg Dering, Andrew Sadowski, Sergey Konyshev, Melissa Penfold, and Ben Parrish. All of whom have offered insightful conversation and instigated new thoughts that aided in the completion and direction of this thesis. I would like to thank my parents for being there for support, offering words of encouragement when the light at the end of the tunnel seemed far and away. And finally, thanks to Jesslyn Starnes, my best friend and compatriot who kept me well fed and inspired through these past couple of years.

Table of Contents

List of Figures

1. Introduction

The Eureka mining district occupies the southern tip of the Battle Mountain – Eureka trend of Carlin-type gold mineralization in east-central Nevada (Figure 1), and contains a series of gold deposits (Nolan, 1962). Numerous geologic investigations of Carlin-type deposits have determined that the geometry of gold orebodies commonly trend parallel to structures, such as folds and faults (Peters, 2004), implying that mineralization is genetically-related to the structures. The Eureka mining district hosts several Carlin-type gold deposits that occur in zones of deformation that are spatially-associated with hydrothermal dissolution, and jasperoidal breccia zones. The purpose of this study is to document structural controls on mineralization within the southern part of the actively-explored and historically-developed Eureka mining district.

Recent advances in understanding the large-scale structural geometry and deformation history of the Eureka district by Long et al. (2012; 2014), and the results of a drilling campaign by Timberline Resources, Corporation (TRC), a junior-scale gold company actively exploring the district, as well as a collaborating partner in this research make a detailed evaluation of the relationships between rock alteration and structural geometry at an economic scale both necessary and timely. Identifying the structural controls on mineralization will assist in generating drill-hole targets for new deposits and may lead to better understanding of Carlin-type mineralization in general.

To address this problem, a 1:10,000-scale geologic map of the region surrounding Lookout Mountain, an active TRC exploration site, has been generated (Figure 2; Plate 1). This map is accompanied by geologic cross-sections, which are supported by surface mapping data and by Timberline's drill-hole data, which are fundamental for constraining unit and alteration

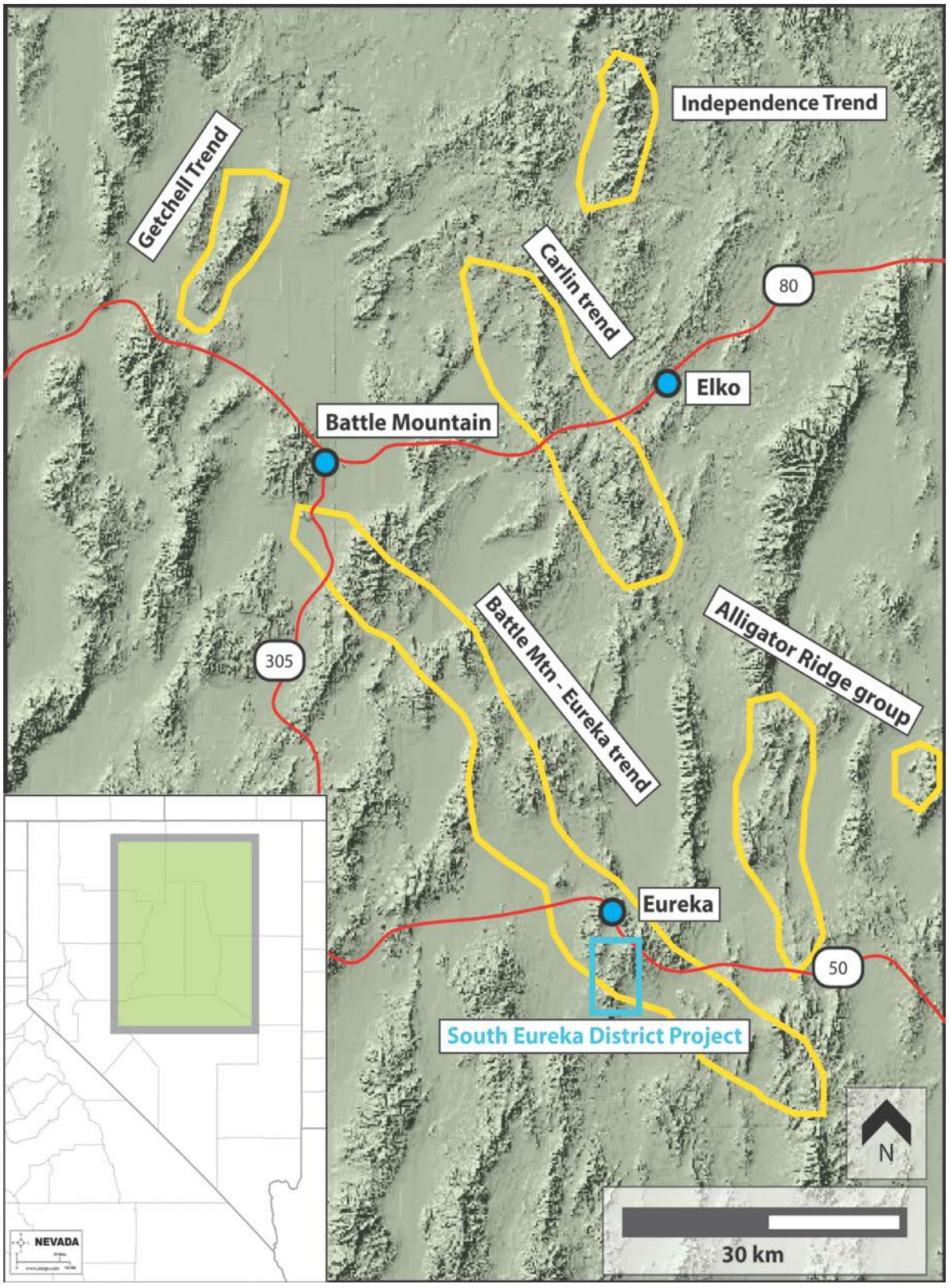

Figure 1. Map showing location of project area with respect to major gold trends in northeastern Nevada. Modified from Peters (2004) and Weber (2005).

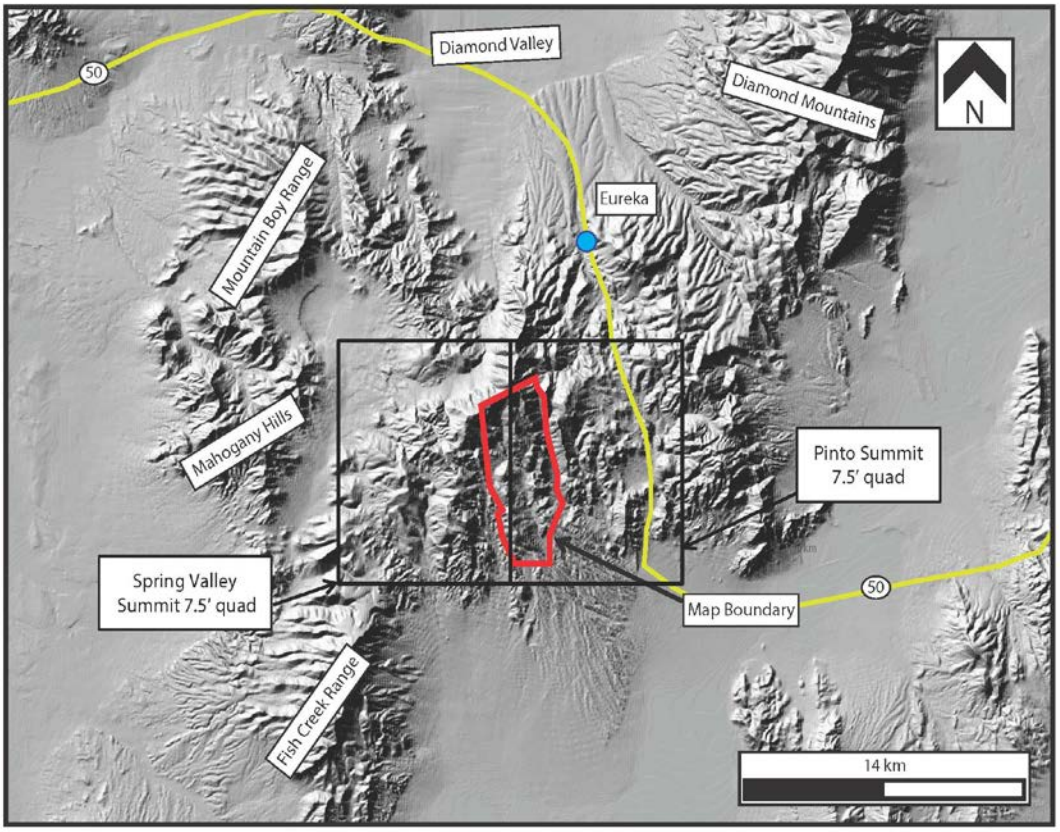

Figure 2. Map showing location of project area, with areas of 7.5' quadrangles shown for scale. Red outline represents map boundary, and yellow line represents U.S. Highway 50.

boundaries at depth. As a second step, the cross-sections are retro-deformed, with motions on extensional faults removed, to assure viable geometries, and to illustrate the pre-extensional (and assumed pre-mineralization) deformation geometry. An Au-grade thickness map was also constructed in order to gain insight into how fault systems may have or may not have influenced the distribution of ore. The map and cross-sections were used to generate a structural model to help elucidate the temporal and spatial evolution of alteration and mineralization, and the degree to which the structural architecture controlled primary hydrothermal fluid pathways

Finally, this project also provides the opportunity to test a structurally-framed model for concentrated mineralization in accommodation zones between overlapping synthetic normal faults. Predictions for mineralization outboard of the primary faults within accommodation and damage zones, as outlined in Micklethwaite et al. (2010), Faulds (2011), and Micklethwaite

(2011), will be tested by cataloging scaling relationships of structures within an accommodation zone within the study area, in conjunction with spatial patterns of alteration obtained through alteration mapping using methods originally developed by the Anaconda Mining Company.

2. Geologic Setting and Tectonic Development

The Eureka mining district, and surrounding region of eastern Nevada, lies within the rifted western margin of the North American craton (Cook and Corboy, 2004). During the early to mid-Paleozoic, the Eureka region was situated on the distal edge of the continental shelf of the Cordilleran passive margin basin, which was a vast carbonate platform (Stewart and Poole, 1974). The Cambrian to Devonian stratigraphic section consists primarily of limestone and dolostone interbedded with shale and sandstone (Figure 4) (e.g., Cook and Corboy, 2004). These carbonate rocks, particularly the Cambrian section, serve as the dominant host rock for mineralization in the district.

During the Late Devonian to Early Mississippian, the Antler orogeny, a contractional deformational event involving eastward-vergent thrusting of deep-water sediments of the Robert's Mountain allochthon over the western edge of the continental shelf, took place to the west of the map area (Figure 3) (Speed and Sleep, 1982). The Eureka region occupied a foreland basin that subsided on the eastern margin of the allochthon, and sediment shed from the eroding highlands shifted the sedimentation-style to the west, depositing carbonaceous silt, sand, and conglomerate. This deposition is represented by a ~ 1.5 km-thick section of Mississippian conglomerate and shale (Nolan et al., 1974).

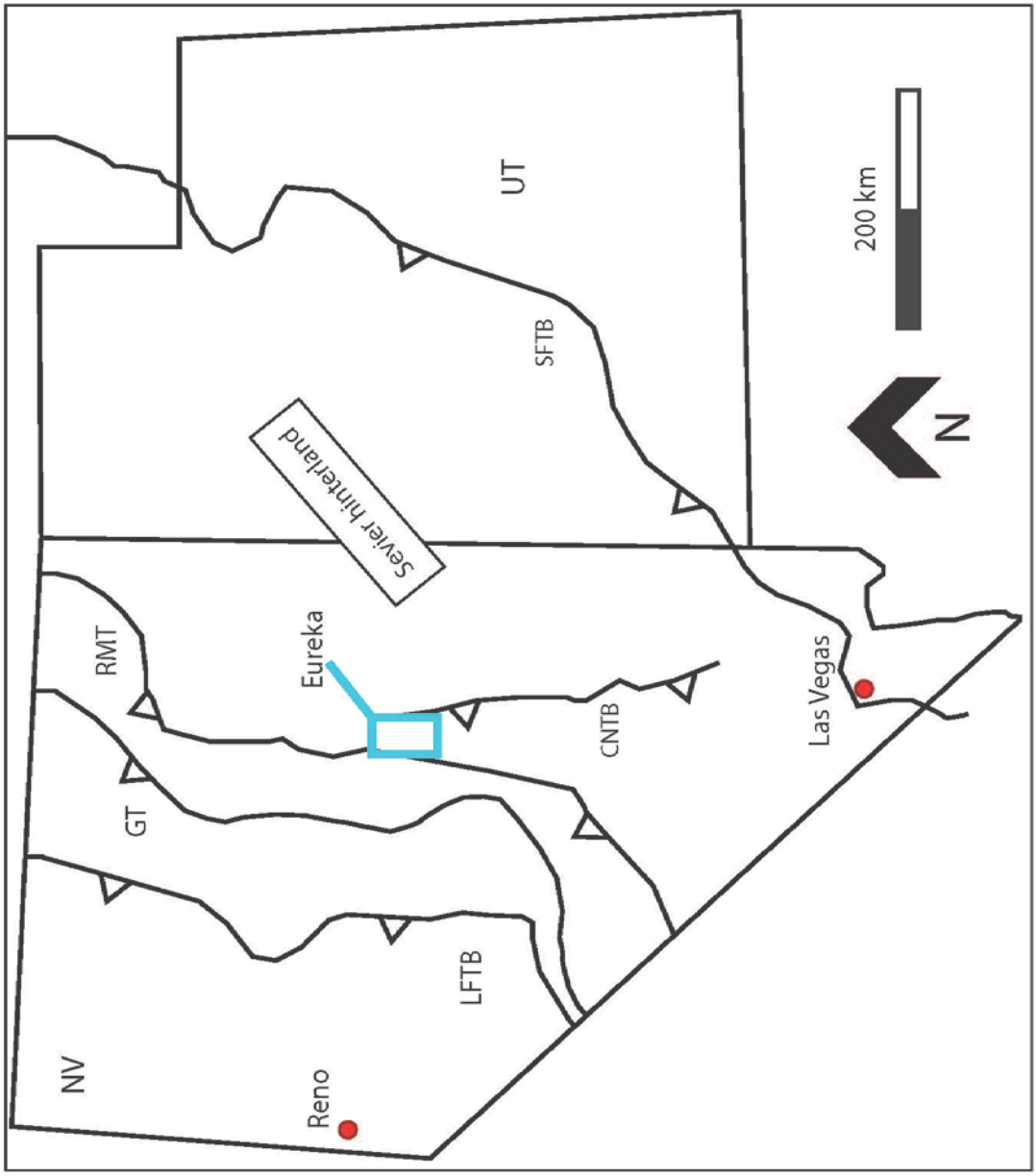

Figure 3. Location of study area relative to Paleozoic and Mesozoic contractional tectonic features. LFTB=Luning Fencemaker thrust belt, GT=Golconda thrust, RMT=Robert's Mountain thrust, CNTB=Central Nevada thrust belt, and SFTB=Sevier fold-and-thrust belt.

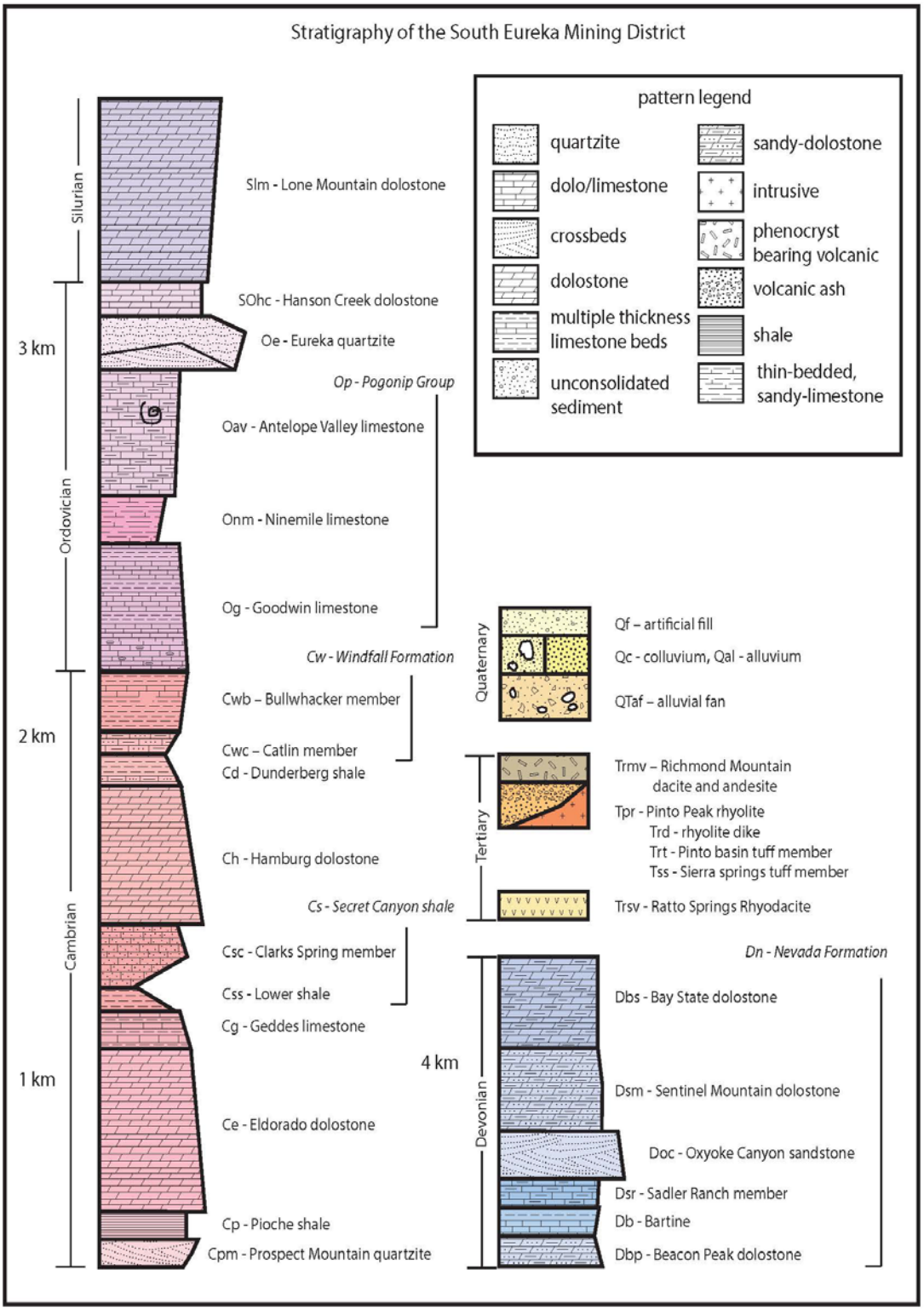

Figure 4. Stratigraphy of the map area

During the Jurassic-Cretaceous Cordilleran orogenic event, the Eureka mining district was

situated between the Jurassic Luning-Fencemaker thrust belt in western Nevada (Oldow, 1984; Wyld, 2002), and the Jurassic-Cretaceous Sevier fold and thrust belt in Utah (Figure 3) (e.g., Armstrong, 1968; DeCelles, 2004). Uplift and erosion during the Sevier orogeny is interpreted to be responsible for the erosion of any Mesozoic strata that would have been deposited prior to eruption of Eocene-Oligocene volcanic rocks (Long, 2012). The Eureka region is situated within the Central Nevada thrust belt (Taylor et al., 1993, Long, 2012), a system of north-striking contractional structures which can be bracketed between Permian and Late Cretaceous (Taylor et al., 2000), and in some places as Early Cretaceous (Long et al., 2014), The Central Nevada thrust belt represents an internal part of the Sevier thrust belt. Long et al. (2014) proposed that the large-scale structure of the Eureka mining district can be explained by Early Cretaceous growth of a regional-scale anticlinal culmination associated with east-vergent motion on the blind Ratto Canyon thrust, which is defined by a Cambrian over Silurian relationship in drill holes beneath Lookout Mountain and Rocky Canyon, in the southern part of the map area (Figure 2).

This Cretaceous contractional deformation was followed by extension along several, large-throw (100's to 1000's of meters) normal faults, which are bracketed between Late Cretaceous and Late Eocene (Long et al., 2014). In the map area, the largest-offset (2,000 – 4,000 meters) normal faults include the Dugout Tunnel and Lookout Mountain faults (Plate 1; Figures 7a-e). These structures are superposed by multiple smaller-scale (10's to 100' of meters offset) normal faults, generally striking north to north-east.

Cenozoic magmatism began at ca. 45 Ma in northeastern Nevada, and was part of a southwestward-migrating belt of silicic magmatism called the Great Basin ignimbrite flare-up. Ignimbrite flare-up magmatism was dominated by andesitic and dacitic lavas and compositionally-similar intrusions (Henry, 2008). In the Eureka region, ignimbrite flare-up rocks

included Late Eocene (~37-33 Ma) silicic ash falls and flows, tuffs, and intrusive volcanic rocks (Nolan et al., 1974; Long et al., 2014).

More recently, Nevada has been the site of regional extension associated with formation of the Basin and Range extensional province. The Basin and Range is a product of the extensional regime introduced by the establishment of the San Andreas transform fault system, the active plate boundary between the North American plate and the Pacific plate, beginning in the Early Miocene (Dickinson, 2006). The map area resides in the Fish Creek Range, and other adjacent modern basins and valleys include the Diamond Mountains, Diamond Valley, the Mountain Boy Range and the Mahogany Hills (Figure 2).

3. Methods

3.1. Geologic and Alteration Mapping

Geologic mapping of the Oswego and Lookout Mountain structural trends (Figure 5) was conducted at a scale of 1:6,000, and is presented here at 1:10,000 (Plate 1). Field-based mapping was supplemented by interpretation of 1:24,000 scale aerial photographs, and was completed on hand-drafted overlays draped over 1:6,000 scale orthoimagery and topography. Drafting of the overlays was completed in ArcMap 10.1 with annotations performed in Adobe Illustrator CS6. The map area is ~3.5 km (east-west) by ~8 km (north-south), and is centered on TRC's Lookout Mountain exploration site, which lies at the northern end of the Fish Creek Range (Figure 2).

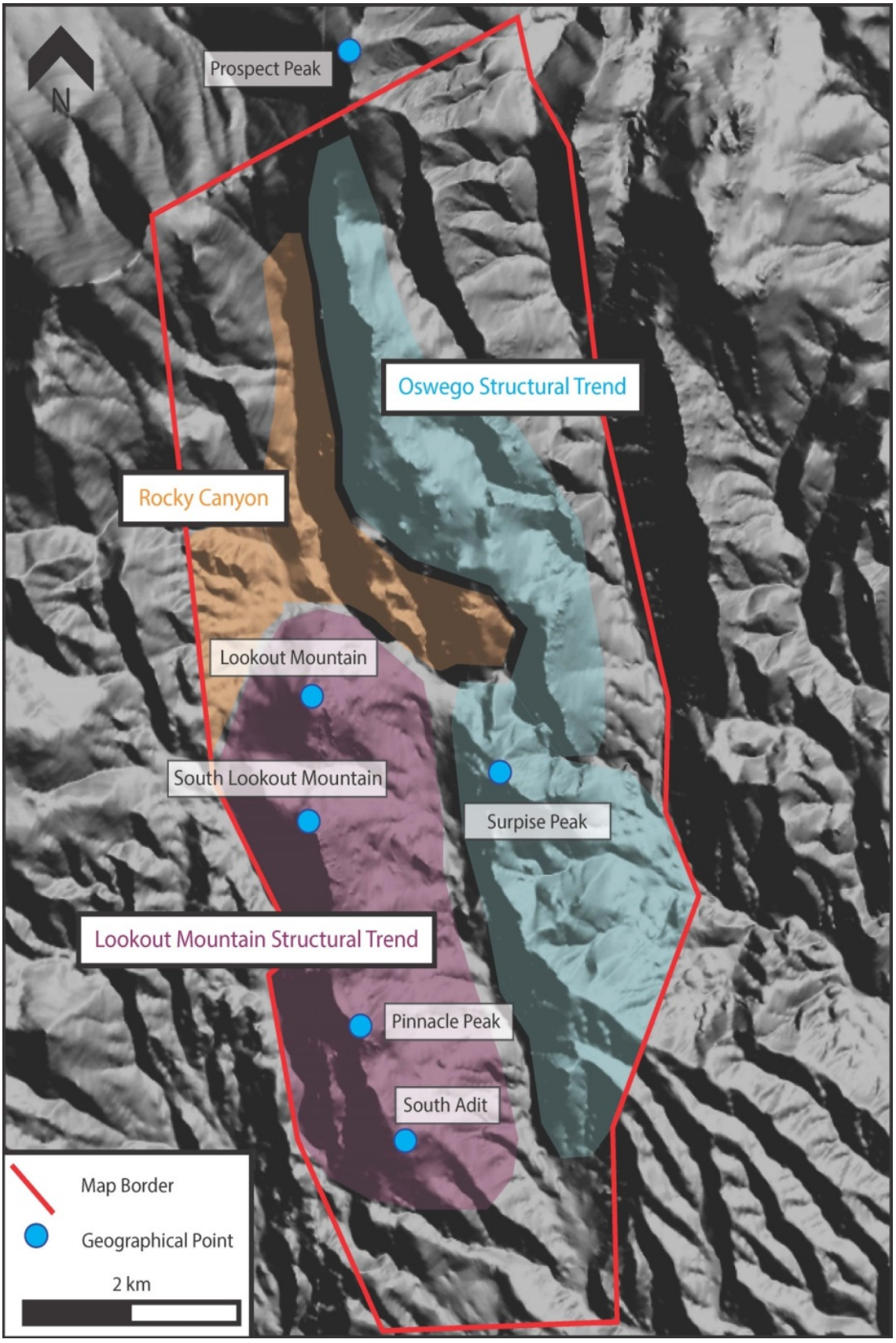

Figure 5. Major structural trends of the project area, including the Lookout Mountain trend (purple), Rocky Canyon system (orange), and Oswego trend (blue). Geographic localities discussed in the text are also labeled.

The location of the study area was chosen based on TRC's existing exploration effort, which is focused on areas of hydrothermal alteration with elevated concentrations of gold. The map boundaries were chosen based on both the spatial extent of the structurally complex Rocky Canyon, Lookout Mountain, and Oswego structural trends (Figure 5), as well the locations of known occurrences of mineralization and exploration targets.

Similarities and differences in textures, outcrop character, weathering character, composition, and local fossil assemblages were used to delineate stratigraphic units (Figure 4), as originally defined by Nolan (1956; 1962) and Nolan et al. (1974).

Alteration mapping was completed as an additional overlay over geologic data using the method originally developed by the Anaconda Mining Company (Einaudi, 1997). The Anaconda mapping scheme is designed to record veining, replacement minerals, ore minerals, sulfide and oxide minerals, and rock alteration in addition to lithology, structure, and geologic contacts, by the use of representative colors, symbols, and shorthand notation (Brimhall, 2006). Specific types of hydrothermal alteration and mineralization products that were mapped include jasperoid (silicification of limestone), decarbonatization of carbonate host rock, carbonization, and argillization, and sulfides (mainly pyrite) and their limonitic weathering products including goethite, hematite, and jarosite. Alteration mapping focused specifically on hydrothermal alteration and mineralization, as it was the primary mode of ore deposition in the study area.

3.2 Cross-Sections

The geologic map is accompanied by five deformed and restored geologic cross-sections (Figures 6a-e), which are constrained by the surface map, data, including the locations of structures and stratigraphic contacts, stratigraphic thicknesses, and apparent dip of strata. In

addition, the cross-sections are constrained by drill-hole data from TRC's ongoing exploration and development campaign, as well as drill-hole data from past exploration campaigns by companies including Newmont, Echo Bay, Barrick, Staccato, and BH Minerals. The cross-sections were drafted along transects perpendicular to the strike of major structures and the dominant regional strike of bedding (Plate 1). The original versions of the cross-sections were drafted by hand, and Adobe Illustrator CS6 was used in drafting and annotating the final sections.

***Figures 6A-E. Cross-Sections; deformed and retro-deformed. A: North Rocky Canyon, B: South Rocky Canyon, C: Lookout Mountain, D: South Lookout Mountain, and E: South Adit. Accompanying Plate 1 in back of thesis.**

Regions of similar apparent dip on the cross-sections were used to define dip-domains. The boundaries between adjacent dip domains were treated as kink-surfaces (e.g., Suppe, 1983), and their orientation was determined by bisecting the intersection angle of the two domains. Dip domains, line lengths, angles, and fault offsets were matched between the deformed and restored cross-sections (Dahlstrom, 1969). In addition, eroded stratigraphy above the modern erosion surface is drafted on the cross-sections. The versions of the cross-sections included in the text of this thesis show both the deformed and restored versions, in order to illustrate fault paragenesis as well as scaling relationships. The versions of the cross-sections in text also omit overlying Quaternary and Tertiary volcanics from the erosion surface for simplicity.

4. Stratigraphy

The map area contains exposures of Paleozoic rocks ranging in age from Cambrian to Devonian, and Cenozoic rocks, including late Eocene volcanics rocks and Quaternary deposits (Figure 4).

Paleozoic rocks

Early Cambrian to Late Devonian rocks are exposed in the map-area, and have a cumulative thickness of ~4.3 km (Figure 4). The true stratigraphic-thickness of shale-dominant units (e.g. Secret Canyon shale, Ninemile Formation, Dunderberg shale) is difficult to determine due to meter-scale folding and faulting.

Lithologic Descriptions

Dn - Nevada Formation (Lower-Middle Devonian)

Dbs - Bay State dolostone member (Middle Devonian): Fossiliferous, fine-medium grained dolostone, which weathers gray to dark gray/brown, and brown to olive-gray when freshly broken. Bedding is locally thin, massive, and uniform (Nolan, 1956). Exhibits abundant characteristic white, elongate, cylindrical "spaghetti" corals (*Cladopora*) as well as abundant, large (2-6 cm) *Stringocephalus* brachiopods. Bedding is more distinct and color is typically lighter and more uniform than Dsm. Forms bluffy and cliffy exposures. 700 feet thick.

Dsm - Sentinel Mountain dolostone member (Middle Devonian): Fine to coarse grained, alternating medium gray-brown/yellow and light-gray weathering dolostone with similar, to darker color on fresh surfaces (Nolan, 1956). Decameter to meter-scale strata-bound color alternation is diagnostic: cm-scale mottling is common in light-gray, thick-bedded, massive dolostone, and the medium gray-brown to yellowish-brown dolostone is generally medium-thick bedded with rare interstitial laminations. Forms rugged, knobby slopes and cliffs; petroliferous when broken. 450-700 feet thick.

Doc - Oxyoke Canyon sandstone member (Middle Devonian): Thick to very thick-bedded, fine to medium-sand grained sized dolomitic sandstone with thin crystalline dolomite interbeds (Nolan, 1956). Weathers light-grey, brown, and tan, and is tan to grey when freshly broken. Interbedded dolomitic quartzose sandstone is fine to coarse-grained, sub-angular to well-rounded, moderately graded, and commonly cross-bedded. Iron-oxide staining parallel with bedforms is common. Forms cliffy to rugged exposures depending on abundance of quartz-sandstone and dolomite. 350 feet thick.

Dsr - Sadler Ranch member (Lower Devonian): Fossiliferous packstone and wackestone, weathers brown-grey to dark-grey, and grey-blue when fresh, and exhibits abundant *Gasterocoma bicuala* two-hole crinoids (Johnson and Lane, 1969). Interbedded with crinoid-rich, finer-grained gray to light gray limestone. Petroliferous odor when broken. Forms subdued slopes. 300 feet thick.

Db - Bartine member of the McColley Canyon Formation (Lower Devonian): Fossiliferous thin- to medium-bedded micrite. Weathers medium-grey to khaki-tan and dark grey when fresh. Abundant fossil hash typically consists of shell and crinoid fragments; fossiliferous interstitial packstones and wackestones are also common. Interbedded with tan to red (liesegang banding) weathering, thin-bedded, silty limestone and siltstone. Outcrops poorly, forming platy, float-covered slopes. Strong petroliferous odor when broken. 125-250 feet thick.

Dbp - Beacon Peak dolomite (Lower Devonian): Fine-medium crystalline to porcellaneous dolostone packstone with interbedded tan, arenaceous, well-laminated bedding. Weathers light gray to white, cream, yellow, olive green, and locally pinkish; fresh surfaces vary from gray, brown-gray to light gray. Medium to thin, well-developed bedding. Locally, rounded dolomite grains are observed, as well as local abundant rounded quartz grains (both clastic in origin) (Nolan, 1956). Forms subdued benches.

Slm - Lone Mountain dolomite (Middle Silurian): Thick bedded, coarse crystalline dolostone. Weathers light-grey to buff, and white to light grey when freshly broken. Recrystallized dolomite rhombohedrons form a diagnostic, coarse, saccharoidal weathering texture. Often silicified and strongly brecciated; commonly vuggy. Forms blocky float and light gray to buff ridges and knobby cliffs. Full stratigraphic thickness not exposed in map area; estimated full thickness from Nolan (1956) is 1,500 feet.

SOhc - Hanson Creek Formation (Upper Ordovician/Lower Silurian): Dark-gray to black, fine-crystalline, massive-weathering dolostone. Often densely fractured and brecciated. Forms centimeter to decimeter scale blocky float and subdued ridges; only exposed in the north-west corner of map area. Full stratigraphic thickness is not exposed in the map area; estimated full thickness from Nolan (1956) is 200 feet.

Oe - Eureka quartzite (Middle Ordovician): White, fine-medium grained, well-graded, well-sorted quartzite; often strongly brecciated. Rare laminations and distinctive cross-bedding in lower part of section; lower contact is sharp, but could be due to structural modification (Long et

al., 2012). Common fracture-controlled iron oxide (red-brown) staining. Coarse-grained sand and interfingering conglomerate lenses are rare. Forms distinct white cliffs and prominent ridges and weathers to large, rounded boulder-sized float. 400 feet thick.

Op - Pogonip Group (Lower-Middle Ordovician)

Oav: Antelope Valley Formation: Thin to thick bedded, bluish gray, fine-grained, wackestone, and packstone with diagnostic very thin to thin tan to yellow silty partings and abundant fossils, both in hash and as whole specimens. Coiled, cm-scale *Maclurites* gastropods shells are diagnostic (Nolan, 1956). Local tan, brown, and white diagenetic chert nodules; less chert in contrast with the Goodwin Formation. Outcrops well, forming blocky ridges and slopes. Interfingering lower contact with Onm; at least 1,000 feet thick.

Onm - Ninemile Formation: Thin-bedded to platy, porcellaneous calcareous shale; weathers tan-green to tan-grey and is olive green to green-tan when freshly broken (Nolan, 1956). Surficial red-brown iron-staining is common. Interbeds of thin, planar bedded gray limestone are common. Distinct from similar units by being arenaceous (Nolan, 1956). Slope forming; does not crop out well. 300-400 feet thick.

Og - Goodwin limestone: Thick, well bedded limestone and wackestone with interbeds of medium bedded, silty, fine–grained limestone weathering light to medium blue-gray

and dark gray when fresh (Nolan, 1956). Gray-brown, white, and black diagenetic chert nodules are common in lower and upper parts of section (Nolan, 1956). Middle part of section primarily consists of thinner-bedded limestone with undulating bedding with common interstitial, thinly bedded silty carbonate layers. Abundant fossil hash; *Kainella* trilobite is diagnostic (Meriam, 1956). Forms rugged, steep slopes and cliffs where strongly brecciated and dolomitized. Upper contact with Onm is gradational. 1,250 feet thick.

Cw - Windfall Formation (Upper Cambrian): Well bedded fossiliferous wackestone and packstone, weathering light gray/brownish-gray to tan/red. Up to 650 feet-thick, but this may be the result of structural thickening by meter-scale folding. Locally divided into:

Cwb – Bullwhacker member: Thin, well-bedded, sandy to shaly fine-grained moderately fossiliferous limestone, weathering tan, light-brown, and red and medium-dark gray when fresh. Contains local interbeds of thinly-laminated, buff-tan-red sandy-shaly partings and thick-bedded, sparse, massive grey-blue limestone beds (Nolan, 1956). Locally contains gray to white diagenetic chert nodules that do not correspond to bedding planes. Fossil hash consists of trilobite, crinoid, and brachiopod fragments. Slope-forming with tan-red platy float; rarely crops out. 400 feet thick.

Cwc – Catlin member: Flaggy, thick to medium bedded, fine-coarse grained medium-gray limestone (Nolan, 1956), weathering tan to buff with common trilobite fossil hash and bioturbation. Alternating bedding with thin-bedded (cm-scale), fissile, sandy-silty

limestone with common tan to red sandy-shaly partings (Nolan, 1956). Diagnostic undulate bedding. Common light gray and dark gray, and black, well-laminated, bedded chert. Approximately 250 feet thick.

Cd - Dunderberg shale member (Upper Cambrian): Very thinly-laminated, non-calcareous shale, which weathers gray to brown/khaki and dark gray/blue when fresh, with diagnostic interbedded cm-scale lenticular limestone (Nolan, 1956), and exhibiting hummocky bedforms. Contemporaneous bedforms in shale form around nodular limestone discs. Bedded limestone often exhibits dense, fine trilobite hash. Less carbonate and silt than Csc. Pervasive meter-scale folding makes determination of true unit thickness difficult. Structural thickness is ca. 350 feet.

Ch - Hamburg dolomite (Middle and Upper Cambrian): Medium to coarse grained, uniform, thick-bedded, gray to brown dolostone weathering brown to light-medium gray. Exhibits mottled white calcite stringers that help define bedding, and white rod-like 'blue bird' stringers (Nolan, 1956). Commonly altered, strongly brecciated, dissolved (Tcb), and/or replaced by amorphous silica (Tjb); can be porous and vuggy due to these alteration processes. Bedding is poorly defined, and dolostone is lighter gray-brown than that of Ce; forms prominent ridges and high-relief cliffs; 1,150 feet thick.

Cs - Secret Canyon shale (Middle Cambrian): Locally consists of an upper limestone member and a lower shale member (Css). Where members cannot be defined, unit is denoted as undifferentiated. Relatively thick shale beds resembling lower Css possibly dispersed throughout

Cs. True thickness is indeterminate due to pervasive meter-scale deformation. Apparent thickness is as much as 700 to 900 feet. Locally divided into:

Csc - Clarks Spring member: Thin-bedded to laminated gray to tan limestone with distinctive contrasting yellow-brown mottling and brown-red argillaceous partings (Nolan, 1956). Limestone is very fine-grained, bio-turbated, and silty, and is tan to blue-gray when fresh. Bedding is laminated to very thinly bedded, and well-stratified. Individual limestone beds are ~2 -7 cm thick. Iron-oxide banding is common. Gradational contact with Css forms platy yellow-green float covered slopes. 500 to 600 feet thick.

Css - Lower shale member: Brown, olive, and tan, calcareous, fossiliferous, fissile shale with rare interbedded, thin-bedded limestone, particularly near the upper contact with Cg. The upper contact with Csc is gradational. Poorly-exposed and slope-forming; often shows up as flakes in float. 200 to 300 feet thick.

Cg - Geddes limestone (Middle Cambrian): Thin to medium-bedded, well-bedded, dark-blue to black carbonaceous limestone with prevalent calcite veins, weathering red/brown to gray, and interbedded with cm-decimeter scale red to tan (iron-oxide) shale beds (Nolan, 1956). Black and distinct bedding is diagnostic. Localized ~2 – 15 cm black chert nodules, are common. Meter-scale, pervasive folding is common and is accompanied by strong fracture controlled white calcite veining. Gradational lower contact with Ce. Outcrops support steep-slopes and bluffs. 200-500 feet thick.

Ce - Eldorado dolomite (Middle Cambrian): Medium-dark gray to blue, very thick-bedded medium to coarse crystalline dolostone, often speckled with common white stringers/spots contrasting with the dark dolostone, giving the unit a diagnostic fenestral ("blue bird") appearance (Nolan, 1956). Dark dolomite locally alternates with light-gray, rough-textured dolostone, which defines bedding, and gives the appearance of alternating light and dark bands, with decameter-scale intervals. Localized meter-scale bands of strong brecciation are common and often correlative with cm-decimeter scale calcite fracture controlled veining. Upper contact with Cg is gradational; contact placed at highest occurrence of massive, thick-bedded blue-gray dolomite. Forms high-relief cliffs; ~1,800 feet thick.

Cp - Pioche shale (Lower Cambrian): Buff-green, and less commonly, red to orange, thin-bedded, micaceous, locally-sandy shale (Nolan, 1956). Generally calcareous with minor arenaceous interbeds. Contains thin interbeds of red-brown (iron-oxide) quartz-arenite, and also thin beds of mottled, dark-blue to gray limestone with abundant trilobite hash, which can closely resemble Oav. 225 ft. thick.

Cpm - Prospect Mountain quartzite (Lower Cambrian): Well-graded, well sorted, white, pink and tan, fine grained quartzite, that weathers white, pink, tan, gray, and brown. Decimeter-scale cross-bedded lamination is diagnostic. Cm to decimeter-scale micaceous to sandy shale interbeds are common in the lower part of the section (Nolan, 1956). Contains rare, thin-bedded pebble conglomerate lenses. Forms sharp cliff and ridge outcrops, with characteristic pink-brown blocky float. No lower contact is exposed; at least 1800 feet thick.

Tertiary rocks

Tertiary collapse breccia and jasperoid are contemporary with Carlin-age mineralization, while the volcanic rocks are dated as Late Eocene (Long et al., 2014).

Tcb - collapse breccia: First-order karsting evident by clasts exhibiting silty horizons, graded bedding, and fluvial re-working. Enhanced by secondary hydrothermal dissolution, consisting of sanded (chemically-rounded, rhombohedral dolomite crystals) dolomite and accumulated non-soluble quartz. Sanding process results in variable amounts of volume loss; often developed within the Hamburg dolostone.

Tj - jasperoid: Fine-grained quartz replacement contemporaneous with dissolution of carbonate host rock; localized in fault zones. Exhibits a fine-sucrosic to smooth crypto-crystalline texture. Ridge and cliff forming; outcrops very well.

Trmv – Richmond Mountain dacite and andesite (Late Eocene): Porphyritic dacite and volcaniclastic deposits and aphanitic andesite lava flows. Flows and dikes weather dark brown to dark red, and are similar to lighter in color on fresh surfaces. Phenocrysts of plagioclase are most common, with lesser hornblende and pyroxene. Contains glassy components (<1 cm to 20 cm in diameter) and abundant vesicles and vugs. Age: 36.16±0.07 Ma, $^{40}Ar/^{39}A$, plagioclase; 36.5±1.3 Ma, K-Ar, hornblende (Long et al., 2014).

Tpr - Pinto Peak rhyolite (Late Eocene): Rhyolite lava flows, dikes, volcanic breccias, and air fall tuff deposits. $^{40}Ar/^{39}Ar$ age of 37.34 ±0.26 Ma (Long et al., 2014).

Tss – Sierra Springs tuff member: Welded tuff, with red to brown matrix with interstitial black fiamme, ranging in size from 2-15 cm (long axis). Exhibits distinct flow banding, with orientation likely related to paleo-topography.

Trt - Pinto Basin Tuff member: Light grey to white, air fall, crystal-lithic lapilli ash tuff. Weathered outcrops can be pale green and pale pink/red with rare biotite phenocrysts. Fluvial reworking yields planar bedding, normally graded, with rare clasts (sand to small gravel) of proximal Paleozoic rock units.

Trd – rhyolite dikes: Decameter to meter scale rhyolitic intrusions. Outcrops weather pale red to medium gray. Dikes exhibit weak to moderate flow banding.

Trsv - Ratto Springs rhyodacite (Late Eocene): Flows and intrusive bodies consisting of 30 - 40 % plagioclase, hornblende, biotite phenocrysts with rare (<5%) quartz. $^{40}Ar/^{39}Ar$ age of ca. 37 Ma (Long et al., 2014).

Quaternary

Qf – artificial fill: Tailings and dump material from open pit mining.

Qal - alluvium: Unconsolidated slope wash debris and river/stream alluvium; exhibits active incision.

Qc - colluvium: Talus and slope-covering unconsolidated sand to large (3 meter) boulder-sized clasts, eroded from proximal bedrock outcrops.

QTaf – **alluvial fan:** Composed of sub-angular to rounded, coarse-sand to cobble clasts of proximal Paleozoic units with carbonate cement. Strongly dissected and deeply incised. Unconsolidated to poorly-consolidated outcrops are rare and usually slope forming.

5. Structural Framework

5.1. Contractional Structures

Thrust faults and folds within the map area record the oldest deformation, forming the structural architecture that was superposed by extensional faults.

Prospect Mountain thrust

An east-vergent, shallowly-dipping thrust fault, the Prospect Mountain thrust (Figure 7) (Long et al., 2014), is observed in the northern area of the map, in the north-end of Rocky Canyon. This fault places lower Cambrian Prospect Mountain quartzite over metamorphosed Cambrian Secret Canyon shale, which defines an older-over-younger relationship. This is the southern continuation of this structure, which is exposed on the north-end of Prospect Mountain, ~1 km north of the map area (Long et al., 2012). Top-to-east offset on the Prospect Mountain thrust is estimated at ~ 850 m (Long et al., 2014). The Prospect Mountain thrust is cut on the west by the Dugout Tunnel normal fault and cut on the east by a down-to-the-east normal fault.

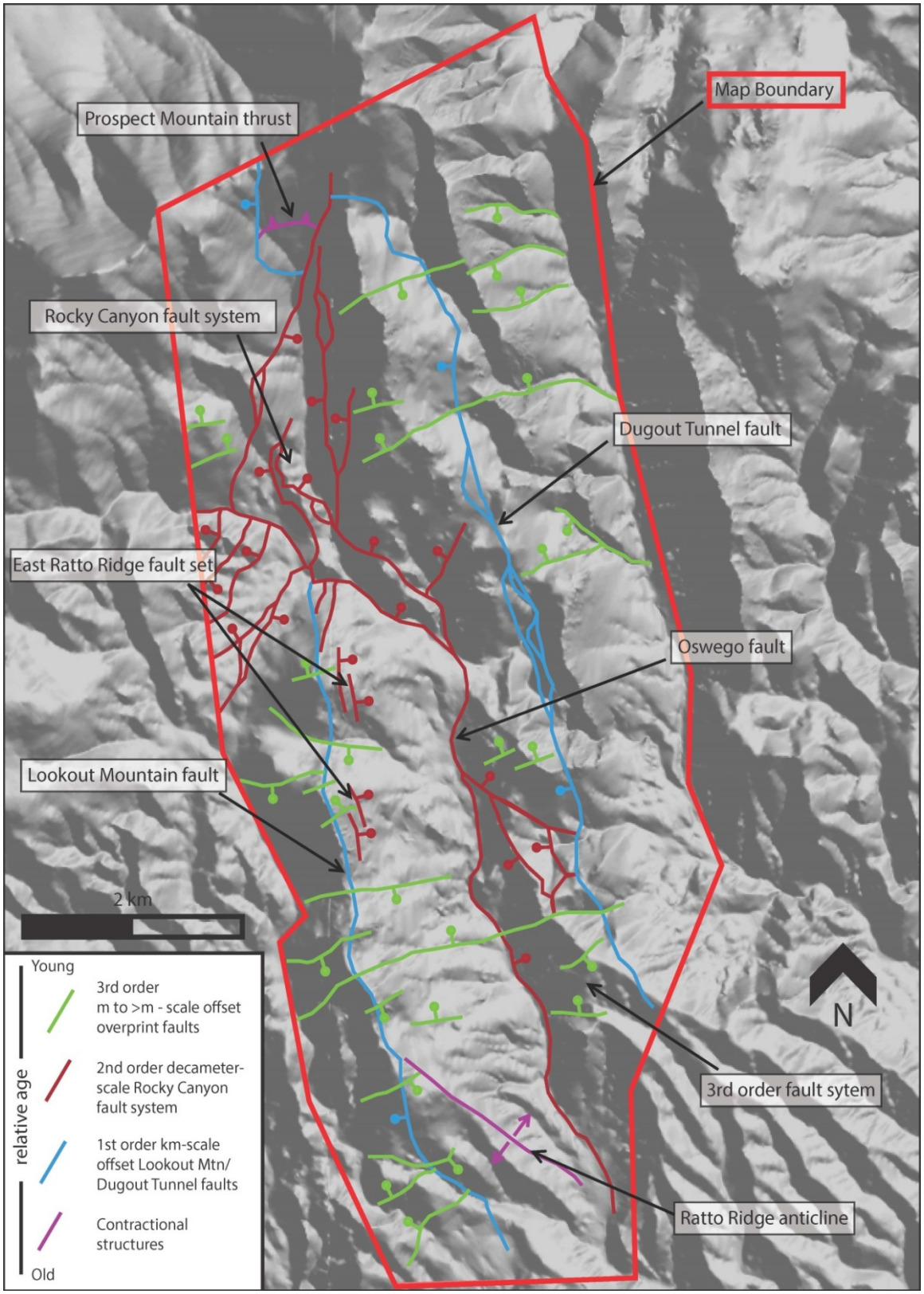

Figure 7. Simplified map of the fault systems of the project area. Faults are classified by order, representing offset amounts: Contractional structures (purple), 1st order, km-scale offset master faults (blue), 2nd-order, decameter-scale offset fault system (red), and 3rd-order, meter- to sub-meter-scale offset overprinting fault system (green).

Ratto Canyon thrust

The Ratto Canyon thrust (Long et al., 2014) is defined by drill-hole data on the east slope of Lookout Mountain, and does not breach the modern erosion surface within the map area. This blind thrust places Cambrian Secret Canyon shale and Cambrian Geddes limestone, over Silurian Lone Mountain dolostone. This older-over-younger relationship is observed in drill holes on the east flank of Lookout Mountain as well as on Ratto Ridge at South Adit (Figure 7, 6C, D, and E). The Ratto Canyon thrust is only observable in drill-hole records, so little is known about its map-scale extent and geometry. Silurian Lone Mountain dolomite and conodonts correlative to the Ordovician Hansen Creek and Ordovician Eureka quartzite were obtained from rocks within the footwall of the thrust, and coincide with the drill-hole lithology interpretations (Long et al., 2014).

Ratto Ridge anticline

A north to north-northeast striking anticline axis can be traced near-parallel with the Lookout Mountain ridgeline (Plate 1; Figure 7). North of Pinnacle Peak, Devonian strata dip gently to the west (~20°) on the west side of the Lookout-Ratto Ridge ridgeline. On the eastern flank of the ridgeline, Cambrian strata typically dip moderately (up to ~50°) to the east. Southeast of South Adit, a northwest-trending anticline axis is observed (Plate 1), and is truncated by a jasperoid outcrop at the ridgeline. This is interpreted to be the southern extent of the Ratto Ridge anticlinal axis. This structure is also demonstrated by opposing strata dip domains across Ratto Ridge (6A, B, C, D, and E). The fold axis appears to have served as a point of crustal weakness that was later exploited by the Lookout Mountain normal fault. Down-to-the-west

motion on this fault has dropped the fold axis of the anticline below the modern erosion surface in the hanging wall of the Lookout Mountain fault.

5.2 Extensional structures

Extensional structures within the map area vary in offset, ranging from meter-scale to multiple kilometers. The largest-throw normal faults include the Lookout Mountain and Dugout Tunnel faults. They are the oldest faults and generally north-striking, and categorized here as 1st -order structures. A 2nd -order set of 10's to 100's of meter-scale offset structures cross-cut the aforementioned 1st-order structures, and typically strike north, northwest, and/or northeast. Lastly, a 3rd -order, meter- to sub-meter-scale offset normal fault system, striking east-northeast, is superimposed on the 1st -order and 2nd -order fault systems, and is interpreted to be the youngest in the field area.

1st order normal faults: Lookout Mountain and Dugout Tunnel faults

Lookout Mountain is bisected by a north striking, steeply (~75-80°) west-dipping normal fault places Devonian strata on the west against steeply east-dipping middle Cambrian strata on the east (Plate 1; Figure 7). The Lookout Mountain fault has ca. 2.3 kilometers of offset in the southern half of the map area (Figures 6C, D, and E). North of Lookout Mountain, the fault disperses into the Rocky Canyon fault system (see description below), a network of 2nd-order structures that forms a complexly-faulted graben in Rocky Canyon. At and south of Lookout Mountain, the Lookout Mountain fault consists of a single, large-offset structure for a map distance of at least 4 km. At the south end of the map area the Lookout Mountain fault is concealed under Quaternary alluvium. According to Cowell (1986), the Lookout Mountain fault

can be traced an additional kilometer to the south where he maps a change in the Lookout Mountain fault's strike from north to east.

The other 1st order normal fault in the map area is the north-striking, steeply (~60°) west-dipping Dugout Tunnel fault, which places shallowly east-dipping Ordovician rocks over steeply east-dipping Cambrian rocks along the full length of the map area (Plate 1; Figures 7, 6A, B, C, and D). At the north end of the map, the fault places Ordovician Hansen Creek dolomite against Cambrian Prospect Mountain quartzite, corresponding to ~3 km of offset. In northern Rocky Canyon, the strike changes to east-west, and the fault cuts nearly perpendicularly up-section in its footwall from the Prospect Mountain quartzite to the Eldorado dolomite. In the adjacent canyon, the Dugout Tunnel fault regains its original north-south strike. The northern half of the Oswego trend is bisected by the Dugout Tunnel fault, which places Ordovician Eureka quartzite and Antelope Valley limestone on the west against Cambrian Eldorado dolomite on the east. Subsidiary synthetic faults that branch off of the master fault place Secret Canyon shale over Eldorado dolomite. South of Surprise Peak the fault bounds a structurally-complex topographic low to the east before becoming concealed, beneath alluvial fan deposits. In Rocky Canyon the Dugout Tunnel fault places unmetamorphosed Ordovician limestone over metamorphosed Cambrian Secret Canyon shale, which is interpreted as a contact aureole associated with Late Cretaceous (ca. 86 Ma) (Long et al., 2014). This offset of the metamorphic aureole brackets the Dugout Tunnel to be no older than ca. 86±0.8 Ma (Long et al., 2014).

Both the Lookout Mountain fault and the Dugout Tunnel fault are overlapped by the Late Eocene (ca. 37 Ma) sub-volcanic unconformity, which provides a youngest motion (Long et al., 2014).

2nd order structures: Oswego fault, Rocky Canyon fault system, and East Ratto Ridge fault system

The down-to-the-east Oswego fault strikes northeast through Rocky Canyon, and strikes north through Ratto Canyon. East of Lookout Mountain, the fault places Ordovician Antelope Valley limestone over Cambrian Dunderberg shale, corresponding to ~900 meters of offset. West of Surprise Peak, this structure bifurcates into two strands. One strand can be traced to the south; the fault loses throw, is only exposed in short segments, and omits little strata, possibly removing parts of the sections of Cambrian Windfall shale or the overlying Ordovician Goodwin limestone. It is inferred to exist in the southern part of the map area due to correlating parallel lineaments of brecciation and mineralization. The second fault strand, just south of Surprise Peak, strikes southeast where it merges with the Dugout Tunnel fault within a complex network of faults (Plate 1; Figure 7). This 2nd –order system can be bracketed as pre-Late Eocene, as it is overlapped by the Late Eocene sub-volcanic unconformity in southern Ratto Canyon (Plate 1).

Another important group of 2nd-order faults is the Rocky Canyon fault system (Figure 7). On the north side of Lookout Mountain, throw on the Lookout Mountain fault decreases by ~900 meters within a north-south map distance of ~ 350 meters. To the north, some of this offset is accommodated by an array of faults that strike northward into Rocky Canyon, here named the Rocky Canyon fault system (Figures 5-7). In Rocky Canyon, a ~900 meter-long horst of Ordovician Pogonip Group rocks is observed, and is bound on the east and west by normal faults that down-drop Silurian and Devonian rocks. On both flanks of Rocky Canyon normal faults place Silurian Lone Mountain dolostone against Ordovician Eureka quartzite and Antelope Valley limestone, defining Rocky Canyon as a complexly-faulted graben. The Ordovician horst is interpreted to be the result of an older down-to-the-east fault being truncated and displaced by a younger down-to-the-west fault (Figure 6B). The faults bounding this horst cannot be mapped further to the north after their traces meet. However, the faults bounding the Rocky Canyon

graben converge on one another in the northern-most part of Rocky Canyon. Here, one fault terminates, or these two faults merge; cover by Quaternary colluvium prevents analysis of their cross-cutting relationship. The Dugout Tunnel fault is cut and offset by the northward continuation of this structure at the northern end of the map area (Plate 1; Figure 7). Along the Rocky Canyon horst, Tertiary dikes intrude along some of these faults, constraining this structural system to the pre-Late Eocene (Figure 8; Plate 1).

Lastly, a set an east-dipping, north-striking faults with decameter-scale offset, can be observed within 1 km of the trace of the 1st -order Lookout Mountain fault, which are here named the East Ratto Ridge fault system. While these faults are not expressed at the surface, they are documented in drill-holes (Figures 6C-E), where they attenuate the Cambrian Hamburg dolomite, and down-drop the Cambrian Dunderberg shale and Windfall Formation. These faults are also overlapped by the sub-volcanic unconformity, bracketing them to pre-Late Eocene.

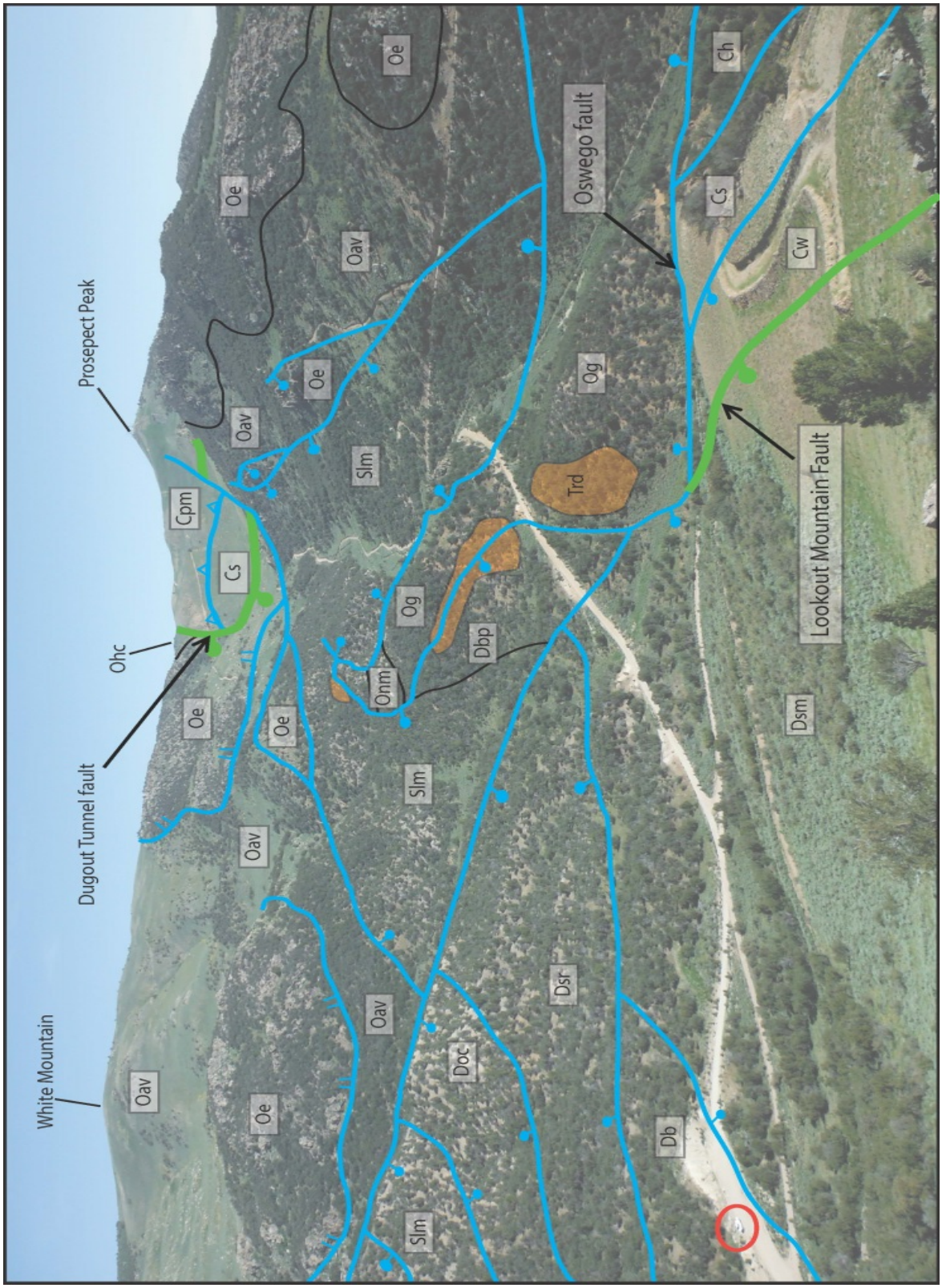

Figure 8. Annotated photograph of Rocky Canyon fault system, looking north from the top of Lookout Mountain. Faults and bedrock contacts are superimposed schematically. Pick-up truck circled in lower-left corner in for scale. Faults are annotated in blue, stratigraphic contacts are shown in black, and transparent-orange polygons indicate Tertiary intrusive rocks.

3rd order structures: younger, small-offset fault set

A set of irregularly-spaced, east to north-east striking normal faults, are distributed over much of the map area, and are exposed primarily in ridgeline outcrops in both the Oswego and Lookout Mountain structural trends (Plate 1; Figure 7). These faults typically exhibit meter- to sub-meter scale offset magnitudes. These small-scale faults cross-cut the large-throw Lookout Mountain and Dugout Tunnel faults and associated jasperoid replacement centered along these structures. Jasperoid replacement bodies and competent stratigraphic units including the Ordovician Eureka quartzite and Cambrian Eldorado dolomite preserve slickenlines that record slip on these faults that indicate dominantly dip-slip motion. Assuming that jasperoid formation was during the Late Eocene, post-dating, or at least penecontemporaneous with the 1st- and 2nd – order structures, than we can postulate these 3rd-order structures to be post-Late Eocene, because they cut and offset the jasperoid bodies.

6. Alteration and Mineralization

6.1 Background: polymetallic and Carlin-type gold deposits

The south Eureka mining district has been a region of mining and mineral exploration for over one-hundred years. The majority of the production has mainly come from oxidized, polymetallic carbonate replacement deposits. Only within the past fifty years has the disseminated, carbonate-hosted Carlin-type gold deposits been recognized and exploited. Both polymetallic carbonate replacement deposits and Carlin-type gold deposits are present in the map area.

Two distinct polymetallic deposits have been characterized. The first of these are hosted within Cambrian and Ordovician rocks, and resemble other polymetallic deposits in the Ruby Hill

and the Mineral Point area, north of the map area. These deposits are spatially coincident and interpreted to be genetically related to Late Cretaceous intrusions dated between 105-108 Ma (Nolan, 1962; Vikre, 1998).

A second suite of polymetallic deposits occur to the west of the map area, and are hosted primarily within Ordovician Pogonip Group carbonates. These are represented through the McCullough's Butte, Reese and Berry, and Dugout Tunnel mines, as well as numerous anomalous mineral occurrences. These latter deposits are postulated to be distal products of the at-depth granite-dike intrusion at McCullough's Butte and Rocky Canyon. For the McCullough's Butte intrusive, Barton (1987) reported an emplacement age, interpreted from K-Ar sampling, of 83.8±1.9 Ma. In Rocky Canyon age-dating of the granite-dikes from samples collected from drill-hole NMC-609C, yielded U-Pb age of 87.42±0.78 Ma (Long et al., 2014).

Polymetallic vein and carbonate replacement deposits are categorized as consisting of lenses, pipes, and veins of iron, lead, zinc, and copper sulfide minerals that are often hosted within carbonate rocks. Carbonate replacement and veining can be both stratigraphically and structurally controlled. These deposits are commonly associated with proximal igneous intrusions, which can also host polymetallic veins (Vikre, 1998). A lack of alteration zoning is common when polymetallic mineralization is hosted within carbonate rock. Where alteration is present limonite-after-sulfide, dolomitization, and localized bodies of jasperoid are the most common. Limonite-after-sulfide can range from robust outcroppings of gossan to fracture controlled-replacement networks. Hydrothermal dolomite and lesser amounts of calcite are also associative to carbonate replacement-bodies correlative to polymetallic deposits (Cox, 1986). Silicification of carbonate rock leading to the formation of jasperoid can occur locally, but generally in lesser abundance relative to Carlin-type gold deposits.

Parallel to Ratto Ridge, disseminated sediment-hosted gold mineralization has been found within the Cambrian Dunderberg and Hamburg Dolomite. These deposits are interpreted to be Carlin-type gold deposits. The Ordovician Pogonip Group outcrops immediately to the north and northeast of the Ratto Ridge resources (Plate 1) and serves as the host rock for additional gold mineralization. Silicification, decarbonatization, and argillization at the subsurface are widespread and extend the entire length of Ratto Ridge (Steininger, 1987). In addition to the deposits along Ratto Ridge, the Oswego Mine directly east of Lookout Mountain exhibits substantial structure controlled gold mineralization. Other similar deposits in the district include the Archimedes mine and the Windfall mine, found north and northeast of the map area, respectively.

Carlin-type gold deposits are epigenetic, disseminated auriferous pyrite deposits characterized by carbonate dissolution, argillic alteration, and silicification of typically calcareous sedimentary rocks, and contain gold as submicroscopic particles in disseminated pyrite, arsenian-pyrite, and/or marcasite. These deposits form along map-scale trends and are both stratigraphically and structurally controlled (Cline et al., 2005).

Three major types of wall-rock hydrothermal alteration have been recognized in Carlin-type deposits: decarbonatization, argillization, and variable silicification in addition to being sulfidized and enriched with gold (Cline et al., 2005). Carbonate rocks are dissolved and locally replaced with quartz. Intense decarbonatization produced collapse breccias significantly increase porosity, permeability, and fluid-rock reaction, leading to the formation of high-grade ore (Bakken, 1990; Emsbo et al., 2003). Wall rocks are argillized where moderately acidic ore fluids reacted with older alumino-silicate minerals and formed assemblages of kaolinite, dickite, and/or illite (Cline et al., 2005). Argillization is related to gold mineralization but is difficult to identify macroscopically. Argillization converts feldspars (regardless if igneous or detrital) into fine-grain

phyllosilicate minerals that include clay minerals, illite, and/or sericite (Arehart, 2003). Since these phyllosilicates are usually fine to very fine-grained, it is difficult to assess the paragenesis of gold and these argillization by-products. Silicification accompanies gold deposition and manifests itself as jasperoid, and, to a lesser extent, by fine quartz druses lining vugs. Jasperoid is spatially coincident with ore at the district-scale, yet can range in gold concentration from high-grade to barren. Jasperoid textures are related to minerals that initially replaced carbonate minerals, thus can indicate an approximate temperature and pressure environment of formation (Lovering, 1972).

Mineralization paragenesis begins with pre-ore events (regional metamorphism and hydrothermal activity) which are responsible for the remobilization of pre-existing minerals, including quartz (manifested as jasperoid), diagenetic pyrite, and calcite common in Paleozoic rocks (Papke, 1984). Gold mineralization is closely associated with hydrothermal arsenian pyrite, marcasite, and pyrite. Late in the Au paragenetic sequence are the arsenic sulfide minerals orpiment and realgar, which postdate the aforementioned hydrothermal sulfides. Significantly later in the sequence barite, stibnite, and ‘late calcite’ are commonly present in open-fracture fillings (Hofstra et al., 2000).

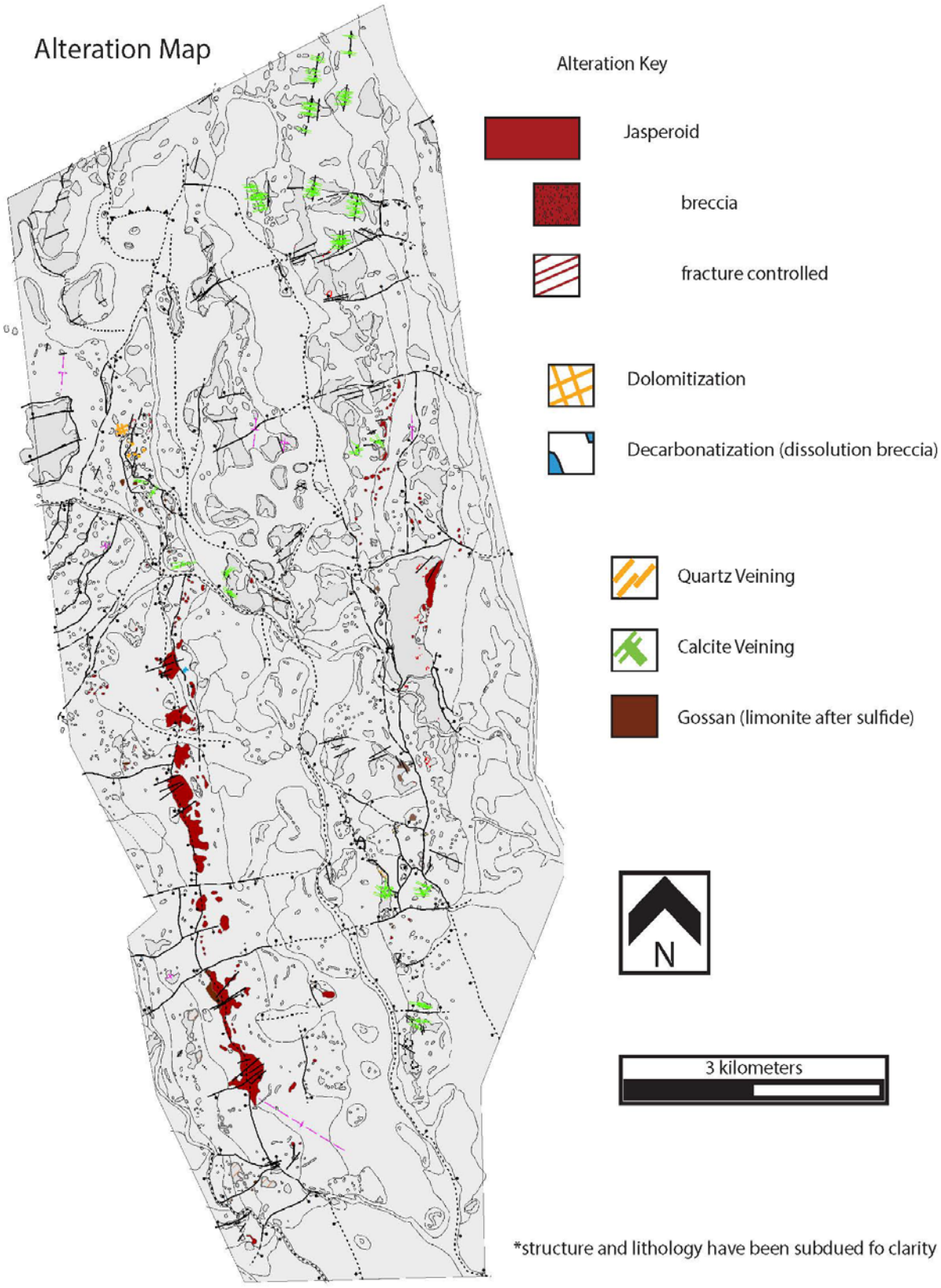

Figure 9. Simplified map of prominent alteration types. Lithology and structural symbols have been grayed-out and subdued for clarity.

6.2 Hydrothermal alteration and mineralization in the map area

In this project, specific categories of rock alteration were mapped including jasperoid (in three stages of replacement: fracture-controlled, breccia, and complete replacement), decarbonatization of carbonate host rock, dolomitization, and advanced stage argillic alteration. The mineralization mapped was limited to limonite (incipient limonite to gossan) and sulfides (pyrite, arsenopyrite, and marcasite), because at the scale that was mapped, this was what could be identified (Figure 9).

The most conspicuous alteration in the map area is the jasperoid replacement bodies. Jasperoid is highly-resistant to weathering in contrast to the easily-weathered decarbonatization. This difference in outcrop weathering pattern generates a bias to jasperoid alteration regarding surface maps of Carlin-type deposits. The competent nature of this replacement silica is responsible for the high-relief topographic expression of Lookout Mountain-Ratto Ridge. Three levels of replacement have been denoted on the map, from incipient to strong they are: fracture-controlled, breccia, and complete replacement (Figure 9). Jasperoid can vary in physical appearance; commonly, a single outcrop can exhibit several distinguishable features (color, replacement texture, etc.) which may or may not be due to the protolith. Within the map area, jasperoid range from brown, brown-gray, dark to light gray, and white. Outcrops of jasperoid are generally highly fractured, and often exhibit multiple stages of structural brecciation. At the hand-lens scale, jasperoid ranges in texture, from a phaneritic saccharoidal texture to aphanitic crypto-crystalline silica. The most common jasperoid host units within the map area are the Cambrian Eldorado dolostone, Cambrian Hamburg dolostone, and the Devonian Sentinel Mountain/Bay State dolostones. While the jasperoid replacing the Cambrian dolostone tend to be brown to dark-gray/brown, the jasperoid replacing the Devonian dolostone is distinctly lighter in color, usually white to gray-white.

Decarbonatization accompanies most carbonate rocks in the map area. This alteration is defined by the removal of carbonate material and manifests itself in outcrop as bulk and local rock volume-loss, obliteration of original rock texture, and increased porosity (vugs, pock-marks, etc.). Due to the scale of this project, decarbonatization was defined in the map area as either present or absent. Also, a biased in the extent of decarbonatization is likely skewed due to the lack of manifestation in outcrop. This alteration was mostly observed in road cuts and pit-walls.

The distribution of limonite was mapped by strength (incipient to strong), and abundance (low to high). Due to the scale of the project, main limonite minerals, goethite, hematite, and jerosite were not differentiated. Limonite was further characterized as being either: fracture-controlled, disseminated, and/or pervasive. Where limonite was both pervasive and strong the term 'gossan' was used, as these relatively competent, massive, vuggy siliceous limonitic bodies were easily distinguishable and cropped out well (Blanchard, 1968). Sulfides were treated in a similar manner and were mapped in the same manner as limonite. The general term 'sulfide' was used in lieu of mapping specific minerals (e.g., pyrite, arsenian pyrite, marcasite, realgar, etc.), in adherence to the scale of the project.

Argillic alteration was mapped only where feldspars or other silicates were completely replaced by clay. Argillic-alteration was only recognized in local igneous bodies which contained phenocrysts. Since most igneous bodies corresponded to dikes emplaced along faults and/or fractures, the argillic alteration marked hydrothermal fluid pathways along these zones.

A zone of rather strong hydrothermal alteration and associated mineralization appears to be centered in Rocky Canyon. It is characterized by dolomitization, milky-quartz veining, gossanous outcrops, and black jasperoid breccia-matrix replacement (Figures 5, 8, and 10B. Much of this mineralization and alteration appears to be different than the Carlin-type mineralization observed along the Lookout Mountain fault to the south. Instead, with black

jasperoid, entrained within the milky quartz veins and the presence of dolomitization, this alteration assemblage resembles that of polymetallic deposits found proximal to the Eureka mining district (Geddes-Bertrand Mine, Ruby Hill Mine, etc.) (Nolan, 1962). This mineralization could be related to the granite dike system located at depth in northern Rocky Canyon (Barton, 1987). These granite dikes have generated a skarn alteration halo that is observed at the surface in northern Rocky Canyon and in drill-hole data. This shale has undergone contact metamorphism to hornfels.

Along Lookout Mountain and Ratto Ridge, disseminated gold is hosted within the Cambrian Hamburg dolostone and an overlaying sealing unit, the Cambrian Dunderberg shale. The mineralization trends parallel with the Lookout Mountain fault trace along the ridgeline. Alteration and mineralization are also observed to the east, in the Oswego structural trend, as well as within the Cambrian Eldorado dolomite to the northern part of the map area.

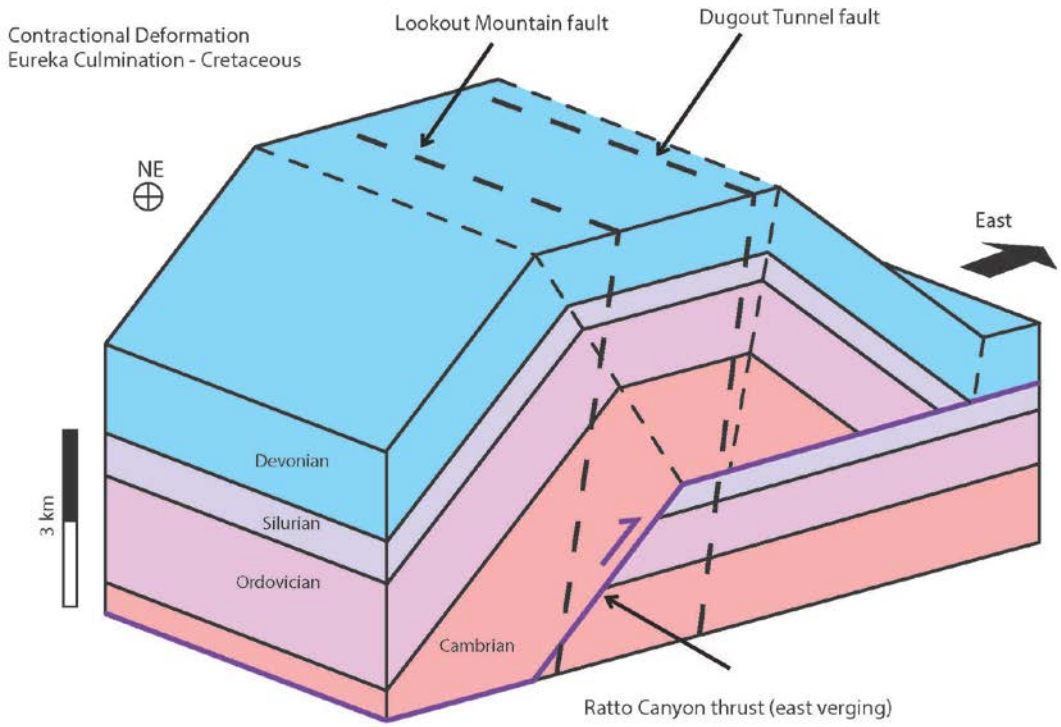

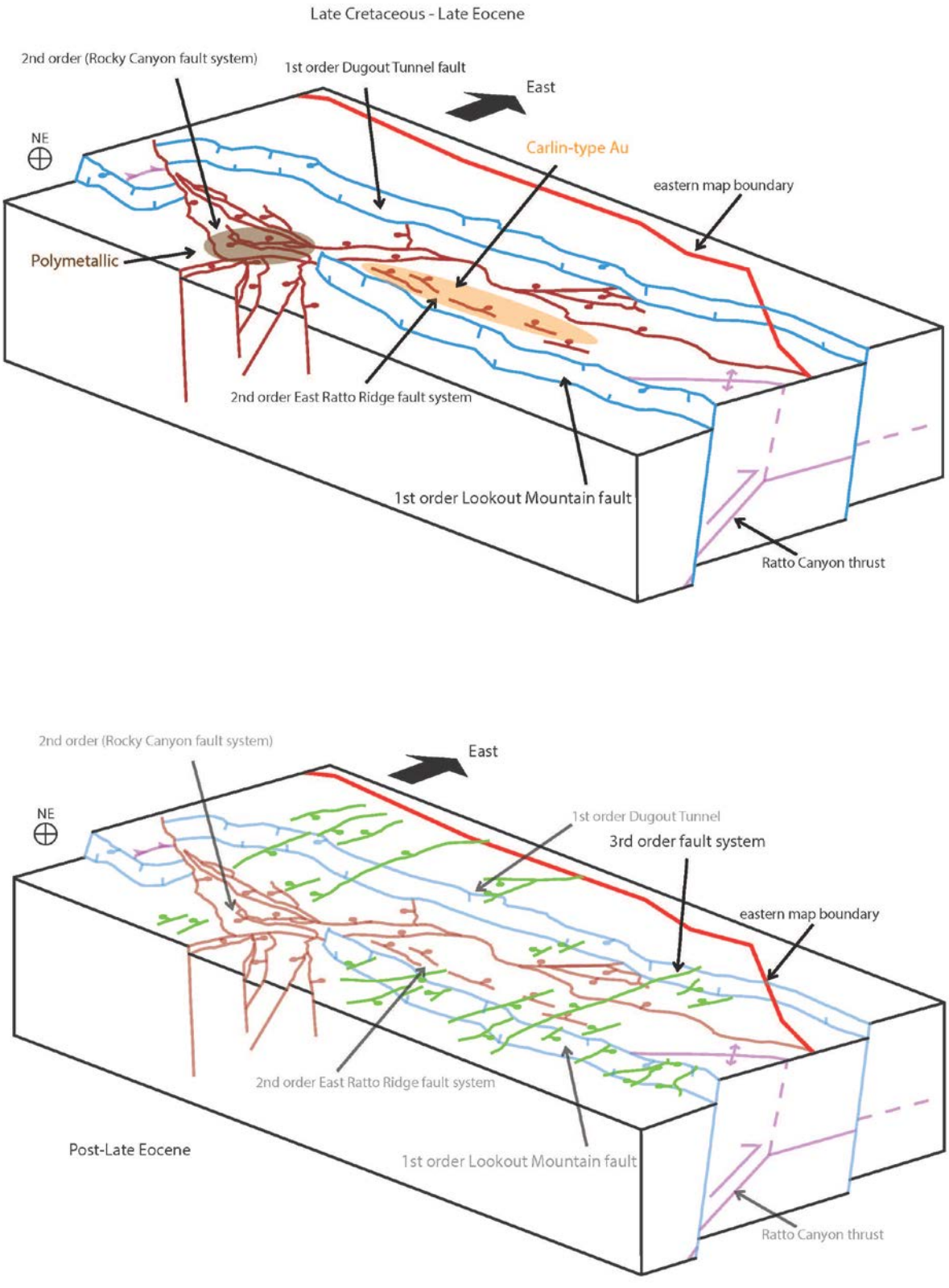

Figure 10. Block diagrams showing the temporal evolution of the structural geometry and mineralization of the map area. A) Late Cretaceous Eureka culmination, Ratto Canyon thrust (purple), and thick dashed lines represent future rupture traces of the 1st-order Lookout Mountain and Dugout Tunnel fault. B) Late Cretaceous – Late Eocene 1st-(blue) and 2nd-order (red) extensional structures. Location of polymetallic (brown) and Carlin-type (gold), shown as transparent halos C) Post-Late Eocene overprinting 3rd-order structures (green).

7. Discussion

7.1 Structural evolution of the map area

The Early Cretaceous construction of the Eureka culmination, a ca. 20 km-wide, 80 km-long anticline (Long et al., 2014), generated the underpinning structural architecture, and set the stage for the superimposed extensional regime (Figure 10A). The map area occupies the approximate center of this regional-scale anticlinal culmination. The culmination is interpreted by Long (2014) as a fault-bend fold, that was constructed by motion on the east-vergent blind Ratto Canyon thrust over a Cambrian to Silurian footwall ramp at depth (Figure 10A).

After construction of the Eureka culmination, motion on 1st- and 2nd-order normal faults took place, and is interpreted here as the result of gravitational collapse of this regional structural high. This faulting can be bracketed between Late Cretaceous (ca. 86 Ma), the age of contact metamorphism in northern Rocky Canyon that is cut by the Dugout Tunnel fault, and Late Eocene (ca. 37 Ma), based on the overlapping relationship of the sub-volcanic unconformity across 1st- and 2nd- order faults in the southern part of the map area (Long et al., 2014). The 1st-order (km-scale offset), large-throw, down-to-the-west Lookout Mountain and Dugout Tunnel faults formed during this event (Figures 7; 10B). Because of a similar strike, steep west-dipping geometry, and amount of throw, the Lookout Mountain fault is interpreted here to be of similar age and origin as the Dugout Tunnel fault. Throughout much of the map area, these two structures strike parallel to one another. The Dugout Tunnel fault maintains an average ~3 km offset throughout the map area until the change in strike to the north. The Lookout Mountain fault maintains both a north strike and ~2.5 km offset through the southern half of the map area, only to abruptly decrease in offset north of Lookout Mountain. Here, this offset is distributed among structures of the 2nd-order Rocky Canyon fault system (Plate 1; Figures 7, 8, 10B), that propagates north into Rocky Canyon. This complex fault system is difficult to trace in northern

Rocky Canyon, but at least one fault is interpreted to offset the Dugout Tunnel fault at the north end of the map area. The Lookout Mountain fault, Dugout Tunnel fault, and Rocky Canyon fault system are interpreted here to be similar in age. This complex array of smaller-scale structures defines an accommodation zone that transfers displacement between the Lookout Mountain and Dugout Tunnel faults (a synthetically-breached relay-ramp, e.g., Faulds and Varga, 1998) (Figure 13) (see section 7.2 below).

An additional set of east-dipping, 2nd-order faults is present within the footwall of the Lookout Mountain fault, defined above as the East Ratto Ridge fault set (Figures 6 and 10B). These antithetic, sub-parallel, decameter-scale offset normal faults are observed only in drill-holes. This fault set is characterized by their steep (~60° ± 10°) eastward dip, and their spatial relationships with the highly-thinned Cambrian Hamburg dolomite that underwent significant decarbonatization (Figure 7D-E). Although the age of these faults relative to the age of Carlin-type mineralization remains enigmatic, overlap of Tertiary volcanics provide evidence for their youngest possible age (Late Eocene). Due to their amount of offset (100's of meters) and geometric characteristics, it is interpreted that these faults are genetically coincident with the 1st - and 2nd -order fault systems.

Finally, a 3rd- order system of east-northeast striking, small-offset (meter- to sub-meter scale) dominantly dip-slip normal faults dissect the map area, offsetting the 1st- and 2nd -order extensional structures (Figure 6, 10C). These faults are generally south-dipping, with only a few dipping to the north. The geometry and amount of offset of these faults were mapped on the jasperoid ridges along the Lookout Mountain and Dugout Tunnel faults, as well as in the Eureka quartzite. Offsets of jasperoid bodies provide an earliest time of fault movement, which is post-Late Eocene.

7.2. Mineralization: spatial patterns and structural controls

Polymetallic alteration and mineralization is evident within uplifted fault-blocks in the 2nd -order Rocky Canyon fault system and is differentiated from Carlin-type alteration by the defining characteristics mentioned above (section 6.2). This mineralization is interpreted to be Late Cretaceous (ca. 86 Ma) in age, because of its spatial association with granite dikes and associated contact metamorphism in northern Rocky Canyon. Therefore, the polymetallic alteration/mineralization is interpreted to pre-date extension, and to have been exhumed as a result of younger motion on the 2nd-order Rocky Canyon fault system.

The timing of mineralization along the Lookout Mountain fault is interpreted to be Late Eocene, synchronous with dated intrusive rocks in the mineralized Lookout Mountain pit (Long et al., in review) (Plate 1). In addition, based on the stratigraphic level of the Late Eocene unconformity across the Lookout Mountain, Dugout Tunnel, Oswego fault, and East Ratto Ridge fault set, and the presence of rhyolitic dikes of presumable Late Eocene age intruding along the Lookout Mountain fault the 1st - and 2nd -order extensional fault systems had to have been completed by the Late Eocene, preceding the Carlin-type mineralization event.

In an attempt to assess structural controls on the spatial patterns of mineralization, a gold-thickness map was constructed (Figure 11). Gold grade-thickness maps are a tool that illustrates the two-dimensional, horizontal spatial representation of Au mineralization intensity. An Au grade-thickness map of the Carlin-type ore-body in the southern half of the map area was drafted (Figure 11), and was generated from data obtained in exploration drilling along Lookout Mountain and South Lookout Mountain by TRC. Since this map is only a two-dimensional representation, and projects concentration data to the location of the drill-hole collar at the surface, even in non-vertical drill-holes, relationships between depth, consistency, and concentration can be difficult to discern. However, educated interpretations can be drawn if the

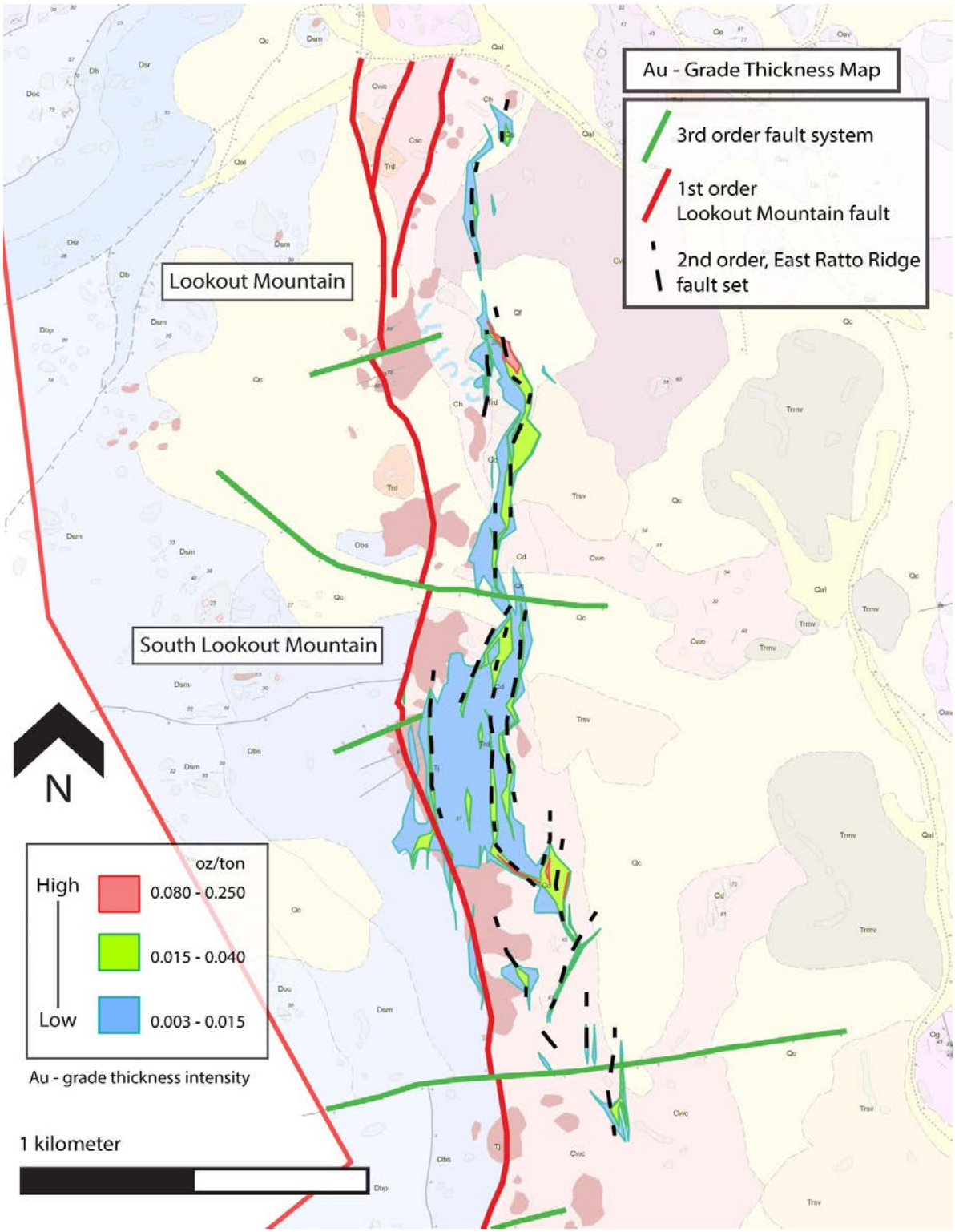

Figure 11. Grade-thickness map of Lookout Mountain. Not shown are traces of individual faults on 2nd-order, east-dipping fault system in the footwall of Lookout Mountain fault. Data supplied by TRC.

following assumptions are made: 1) we have access to total depth of drill-holes, 2) holes are drilled through the zone of mineralization; and 3) the distribution of mineralization can be attributed to an ore-deposit type. Additionally, utilizing TRC's cross-sections drawn perpendicular to the mineralized trend (e.g., Figure 12), the geometry of the ore-body at depth can be illustrated, to provide support to the 2-D patterns illustrated on the gold-thickness.

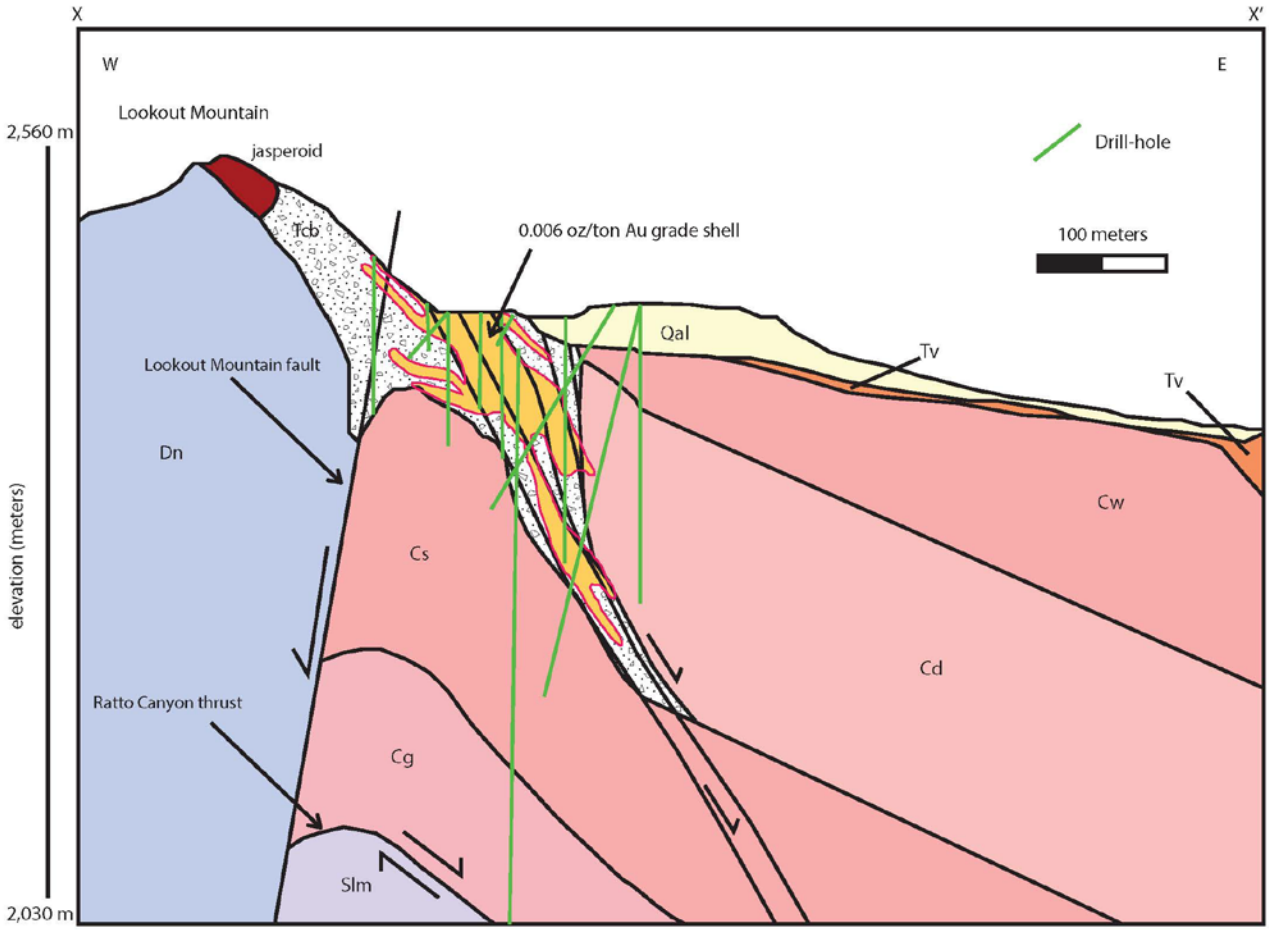

Figure 12. Annotated cross-section, drafted by Timberline Resources Corporation, showing the geometry of Au mineralization at depth, and illustrating the system of 2nd- order antithetic faults in the footwall of the LMF.

In the map area, zones of elevated grade thickness run sub-parallel to the strike of the Lookout Mountain fault, with the majority of the zones confined to the footwall (Figure 13). The zones of moderate grade thickness have a distinct linear geometry, which trends sub-parallel to parallel to the Lookout Mountain fault. This pattern outlines the map pattern of the East Ratto Ridge fault set, an antithetic, 2nd -order fault system within the altered ground sub-surface. The existence of these faults is supported in drill-hole data (Figure 12). The close proximity from

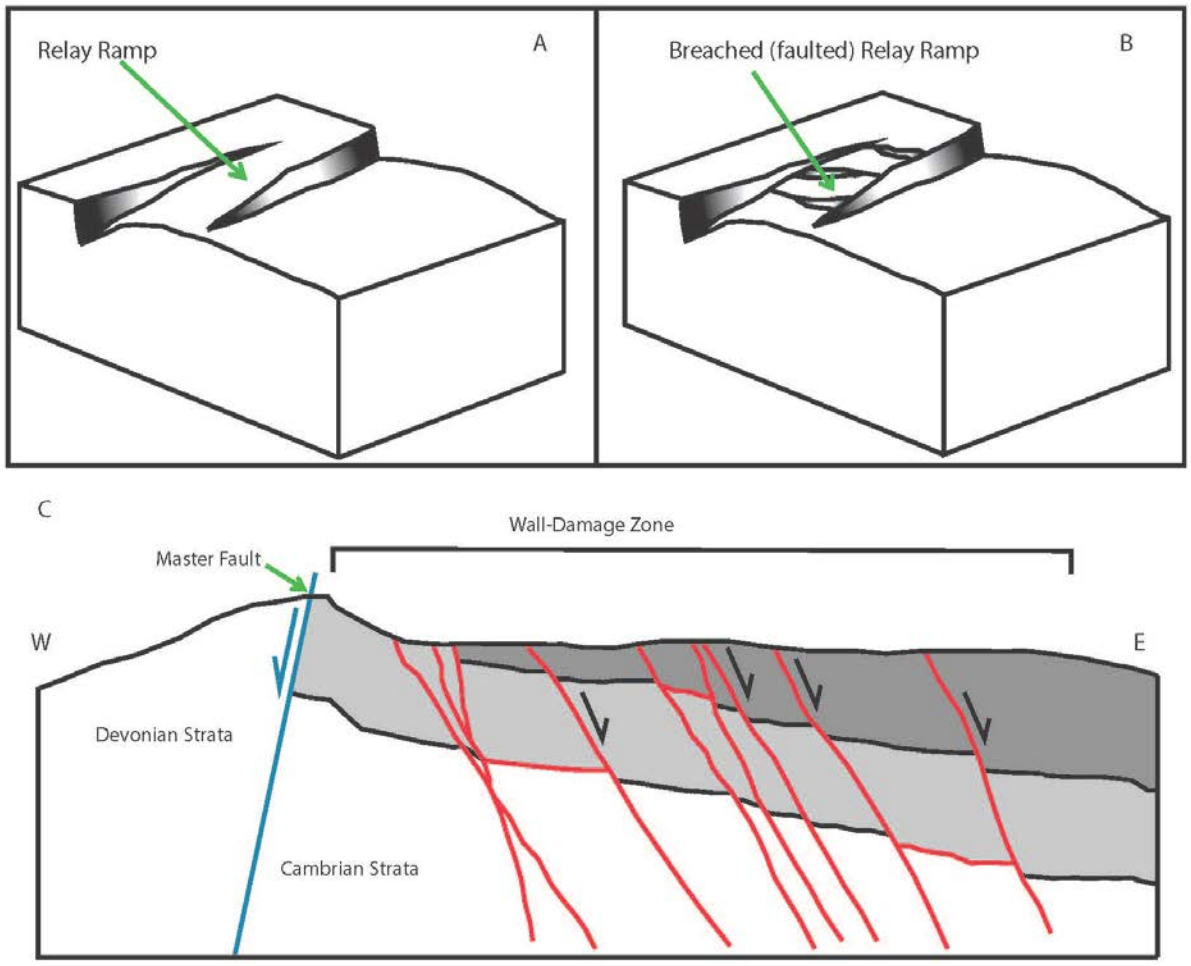

Figure 13. Schematic breached (faulted) relay ramp accommodation zone. Green arrow points to relay ramp between two 1st-order, synthetic normal faults. Modified from Faulds and Varga (1998).

Figure 14. Schematic diagram of a wall-damage zone of a master fault (blue) exhibiting opposing dips of antithetic faults (red). Modified from Micklethwaite (2010).

one fault to another allowed for increased permeability due to interconnected network of damage zones (Caine et al., 1996). These 2nd-order faults are interpreted to have been integral for creating zones of localized fluid flow and thus, were favorable sites for mineralization. The majority of the mineralization related to the 1st -order Lookout Mountain fault are spatially coincident with, and were strongly controlled by, this 2nd -order antithetic fault system.

7.3 Testing predictions of mineralization in accommodation zones

An accommodation zone is defined as an area of faulting and/or folding that serves to transfers slip between larger structures (Faulds and Varga, 1998). These zones manifest themselves as belts of overlapping fault terminations and can separate systems of either synthetic faults or antithetic faults (Faulds and Varga, 1998). The majority of the map area occupies such an accommodation zone (Figure 7 and 10B); the 1st -order Lookout Mountain fault and Dugout Tunnel are interpreted to be genetically linked, and due to style of deformation, respective geometries, and spatial distribution of offset, the 2nd –order Rocky Canyon fault system is interpreted to represent an accommodation zone that connects them (Figure 13). Specifically, this accommodation zone represents a synthetically-breached relay ramp, using the terminology of Faulds and Varga (1998).

Wall-damage and linking-damage zone structures are proposed to control the migration of fluids and influence the localization of gold mineralization within accommodation zones (Figure 14) (Micklethwaite, 2011). A damage zone is defined as the volume of deformed wall rocks around a fault surface that results from the propagation, initiation, and the build-up of slip along faults. Damage zones are classified into different geometric types depending on their location relative to the master faults in an accommodation zone (Kim et al., 2004). Tip-damage

zones are developed at the tips of faults, linking-damage zones form where adjacent fault segments interact and link (e.g., stepovers), and wall-damage zones represent faulting and fracturing in the proximal wall-rock region of a fault. TRC's drilling campaign has revealed closely-spaced concentrations of hydrothermal dissolution of carbonate, accompanying silicification, and the formation of jasperoid bodies along the large-throw Lookout Mountain fault with gold-mineralization localized in the footwall (Figures 10B, 11, and 12). The footwall of the 1st -order Lookout Mountain fault contains a set of 2nd -order east-dipping faults (East Ratto Ridge fault set) which are spatially coincident with this alteration and mineralization (Figure 10C, 11, and 12). It is interpreted that these 2nd -order antithetic (to the Lookout Mountain fault) faults represent a wall-damage zone in the footwall of the 1st –order Lookout Mountain fault, and thus are responsible for the requisite ground preparation for the formation of the Carlin-type ore-deposit.

8 Conclusions

1. The Early Cretaceous construction of the Eureka culmination generated the underpinning structural architecture for subsequent gravitational collapse which was manifested by the 1st- and 2nd order extensional fault systems, which are post ca. 86 Ma (age of granite dikes and contact aureole), and pre-Late Eocene. The 2nd- and 1st-order faults are interpreted to be genetically related, defining a zone of accommodation of 2nd-order faults that transfer displacement between two synthetic 1st-order structures (i.e., a synthetically breached relay-ramp, e.g., Faulds and Varga, 1998). Finally, a 3rd -order fault set cross-cuts all earlier structures, and is presumably post-late Eocene.

2. Polymetallic alteration in northern Rocky Canyon is interpreted to be associated with Late Cretaceous granite dike system at depth. Rocks that underwent polymetallic alteration and mineralization were later exhumed by structures of the Rocky Canyon fault system.

3. The timing of Carlin-type mineralization along the Lookout Mountain fault is interpreted to be Late Eocene, synchronous with intrusive rocks in the mineralized Lookout Mountain pit. The majority of the mineralization related to the 1st -order Lookout Mountain fault is actually off-fault, and is spatially coincident with the 2nd-order, antithetic East Ratto Ridge fault system. This fault system is interpreted as the primary structural control for localizing fluid flow and formation of the Carlin-type ore body.

4. Wall-damage zone structures are proposed control the migration of fluids and influence the localization of gold mineralization in accommodation zones. The 2nd-order East Ratto Ridge fault system, which is antithetic to and in the immediate footwall of the 1st-order Lookout Mountain fault, is interpreted to represent a footwall wall-damage zone. Therefore, mineralization patterns in the south Eureka district confirm predictions for structural controls on mineralization in accommodation zones.

References Cited

Arehart, G., and Chakurian, A., 2003, Evaluation of radioisotope dating of Carlin-type deposits in the Great Basin, western North America, and implications for deposit genesis: Economic Geology, v. 98, p. 235–248.

Armstrong, R.L., 1968, Sevier orogenic belt in Nevada and Utah: Geological Society of America Bulletin, v. 79, p. 429-458.3.

Bakken B.M., 1990, Gold mineralization, wall-rock alteration and the geochemical evolution of the hydrothermal system in the main ore body, Carlin Mine, Nevada: Unpublished Ph.D. thesis, Stanford, CA, Stanford University, 236 p.

Best, M.G., Barr, D.L., Christiansen, E.H., Gromme, S., Deino, A.L., and Tingey, D.G., 2009, The Great Basin Altiplano during the middle Cenozoic ignimbrite flareup: insights from volcanic rocks: International Geology Review, v. 51, p. 589-633.

Brimhall, G. H, Dilles, John, Proffett, J., 2006, The Role of Geological Mapping in Mineral Exploration in Wealth Creation in the Minerals Industry, Special Publication 12, Anniversary Publications of the Society of Economic Geologists, p. 221-241

Blanchard, R., 1968. Interpretation of leached outcrops. Nevada Bureau of Mines and Geolgy. Bulletin 66 (196 pp).

Caine, J., Evans, J., and Forster, C., 1996, Fault zone architecture and permeability structure: Geology, p. 1025–1028.

Cline, J.S., Hofstra, A.H., Muntean, J., Tosdal, R.M., and Hickey, K.A., 2005, Carlin-type gold deposits in Nevada: critical geologic characteristics and viable models: Society of Economic Geologists Abstracts with Programs, 100th anniversary volume, p. 451-484.

Cook, H.E., and Corboy, J.E., 2004, Great Basin Paleozoic carbonate platform: facies, facies transitions, depositional models, platform architecture, sequence stratigraphy, and predictive mineral host models: U.S.G.S. Open-File Report 2004-1078, 129 p.

Cox, D., and Singer, D., 1986, Mineral deposit models: U.S. Geological Survey, Bulletin 1693

Dahlstrom, C.D.A., 1969, Balanced cross sections: Canadian Journal of Earth Sciences, v. 6, p. 743–757, doi: 10.1139/e69-069.

DeCelles, P.G., and Coogan, J.C., 2006, Regional structure and kinematic history of the Sevier fold-and-thrust belt, central Utah: Geological Society of America Bulletin, v. 118, p. 841-864.

Dickinson, W.R., 2002, The Basin and Range Province as a composite extensional domain: International Geology Review, v. 44, p. 1–38.

Dilles, P.A., Wright, W.A., Monteleone, S.E., Russell, K.D., Marlowe, K.E.,Wood, R.A., and Margolis, J., 1996, The geology of the West Archimedes deposit: A new gold discovery in the Eureka mining district, Eureka County, Nevada, in Coyner, A.R., and Fahey, P.L., eds., Geology and Ore Deposits of the American Cordillera: Symposium Proceedings: Reno, Geological Society of Nevada, p. 159–171.

Emsbo P., and Hofstra, A.H., 2003, Origin and significance of post dissolution collapse breccias cemented with calcite and barite at the Meikle gold deposit, northern Carlin trend, Nevada: ECONOMIC GEOLOGY, v. 98, p. 1243–1252.

Faulds, J. E., and Varga, R. J., 1998, The role of accommodation zones and transfer zones in the regional segmentation of extended terranes, *in* Faulds, J. E., and Stewart, J. H., eds., Accommodation zones and transfer zones: Regional segmentation of the Basin and Range province: Geological Society of America Special Paper 323, p. 1–45.

Faulds, J., and Hinz, N., 2011, Assessment of favorable structural settings of geothermal systems in the Great Basin, Western USA: Geothermal …, v. 35.

Henry, C.D., 2008, Ash-flow tuffs and paleovalleys in northeastern Nevada: Implications for Eocene paleogeography and extension in the Sevier hinterland, northern Great Basin: Geosphere, v. 4, p. 1, doi: 10.1130/GES00122.1.

Hofstra, A.H., and Cline, J.S., 2000, Characteristics and models for Carlin-type gold deposits, in, Thompson, T.B., ed., Society of Economic Geology Reviews, v. 13, Denver, CO, p. 163-220.

Ketner, K.B., Murchey, B.L., Stamm, R.G., Wardlaw, B.R., 1993. Paleozoic and Mesozoic rocks of Mount Icabod and Dorsey Canyon, Elko County, Nevada—evidence for Post-early Triassic emplacement of the Roberts Mountains and Golconda allochthons. U.S. Geological Survey Bulletin 1988, 12.

Kim, Y.-S., Peacock, D.C.., and Sanderson, D.J., 2004, Fault damage zones: Journal of Structural Geology, v. 26, p. 503–517, doi: 10.1016/j.jsg.2003.08.002.

Long, S.P., Henry, C.D., Muntean, J.H., Edmondo, G.P., and Thomas, R.D., 2012, Preliminary geologic map of the southern Eureka mining district, Eureka and White Pine Counties, Nevada: Nevada Bureau of Mines and Geology Open-File Report 12-6, 1:24,000-scale, 2 plates.

Long, S.P., Henry, C.D., Muntean, J.L., Edmondo, G.P., and Cassel, E.J., in revision, Early Cretaceous construction of a structural culmination, Eureka, Nevada, U.S.A.: implications for out-of-sequence deformation in the Sevier hinterland: Geosphere.

Lovering, T.B., 1972, Jasperoid in the United States-Its Characteristics, Origin, and Economic Significance: U.S. Geological Survey Professional Paper 710.

Micklethwaite, S., 2011, Fault-induced damage controlling the formation of Carlin-type ore deposits; Geological Society of Nevada, p. 711-721

Micklethwaite, S., Sheldon, H.A. and Baker, T., 2010, Active fault and shear processes and their implications for mineral deposit formation and discovery; Journal of Structural Geology, v. 32, p. 151-165.

Muntean, J.L., Cline, J.S., Simon, A.C., and Longo, A. a., 2011, Magmatic–hydrothermal origin of Nevada's Carlin-type gold deposits: Nature Geoscience, v. 4, p. 122–127, doi: 10.1038/ngeo1064.

Nolan, T.B., Merriam, C.W., and Williams, J.S., 1956, The stratigraphic section in the vicinity of Eureka, Nevada: U.S. Geological Survey Professional Paper 276, p. 77.

Nolan, T.B., 1962, The Eureka Mining District, Nevada: U.S. Geological Survey Professional Paper 406, p. 78.

Nolan, T.B., Merriam, C.W., and Brew, D.A., 1971, Geologic map of the Eureka quadrangle, Eureka and White Pine counties, Nevada: U.S. Geological Survey Miscellaneous Investigations Series, Map I-612: 1:31,680-scale, 8 p., 2 plates.

Nolan, T.B., Merriam, C.W., and Blake, M.C., Jr., 1974, Geologic map of the Pinto Summit quadrangle, Eureka and White Pine counties, Nevada: U.S. Geological Survey Miscellaneous Investigations Series, Map I-793: 1:31,680-scale, 14 p., 2 plates.

Oldow, J.S., 1984, Evolution of a late Mesozoic back-arc fold and thrust belt, northwestern Great Basin, U.S.A.: Tectonophysics, v. 102, p. 245–274, doi: 10.1016/0040-1951(84)90016-7.

Papke, K.G., 1984, Barite in Nevada: Nevada Bureau of Mines and Geology

Bulletin 98, 125 p.

Peters, S.G., 2004, Syn-deformational features of Carlin-type Au deposits: Journal of Structural Geology, v.26, p.1007-1023.

Roberts, R.J., Hotz, P.E., Gilluly, J., Ferguson, H.G., 1958. Paleozoic rocks of north-central Nevada. American Association of Petroleum Geologists Bulletin 42 (12), 2813–2857.

Silberling, N.J., 1975. Age relationships of the Golconda thrust fault, Sonoma Range, north-central Nevada: Geological Society of America Special Paper 163, 28.

Speed, R. C., and Sleep, N. H., 1982, Antler orogeny and foreland basin: A model: Geological Society of America Bulletin, v. 93, p. 815-828

Steininger, R. C., Klessig, P. J., and Young, T. H., 1987, Geology of the Ratto Canyon gold deposits, Eureka County, Nevada, in Johnson, J. I., (ed.), Bulk Mineable Precious Metal Deposits of the Western United States, Guidebook for Field Trips, p. 293-304.

Suppe, J., 1983, Geometry and kinematics of fault-bend folding: American Journal of Science, v. 283, p. 684–721, doi:10.2475/ajs.283.7.684.

Taylor, W.J., Bartley, J.M., Fryxell, J.E., Schmitt, J., and Vandervoort, D.S., 1993, Mesozoic Central Nevada thrust belt, *in* Lahren, M.M., Trexler, J.H., and Spinosa, C., eds., Crustal Evolution of the Great Basin and the Sierra Nevada: Geological Society of America Cordilleran/Rocky Mountain Sections Field Trip Guidebook: Boulder, p. 57-96.

Taylor, W.J., Bartley, J.M., Martin, M.W, Geissman, J.W., Walker, J.D., Armstrong, P.A., and Fryxell, J.E., 2000, Relations between hinterland and foreland shortening: Sevier orogeny, central North American Cordillera: Tectonics, v. 19, no. 6, p. 1124-1143.

Vikre, P.G., Derby, J., I, M.G., Phillips, D.L., Jarvis, R., and Long, J., 1998. Intrusion related, polymetallic carbonate replacement bodies in the Eureka district, Eureka County, Nevada Mines Nevada Bureau of Mines and Geology:

Geologic Map of the Lookout Mountain and Oswego Structural Trends, South Eureka Mining District

Russell V. Di Fiori, Sean P. Long, John L. Muntean, and Gary Edmondo
2014

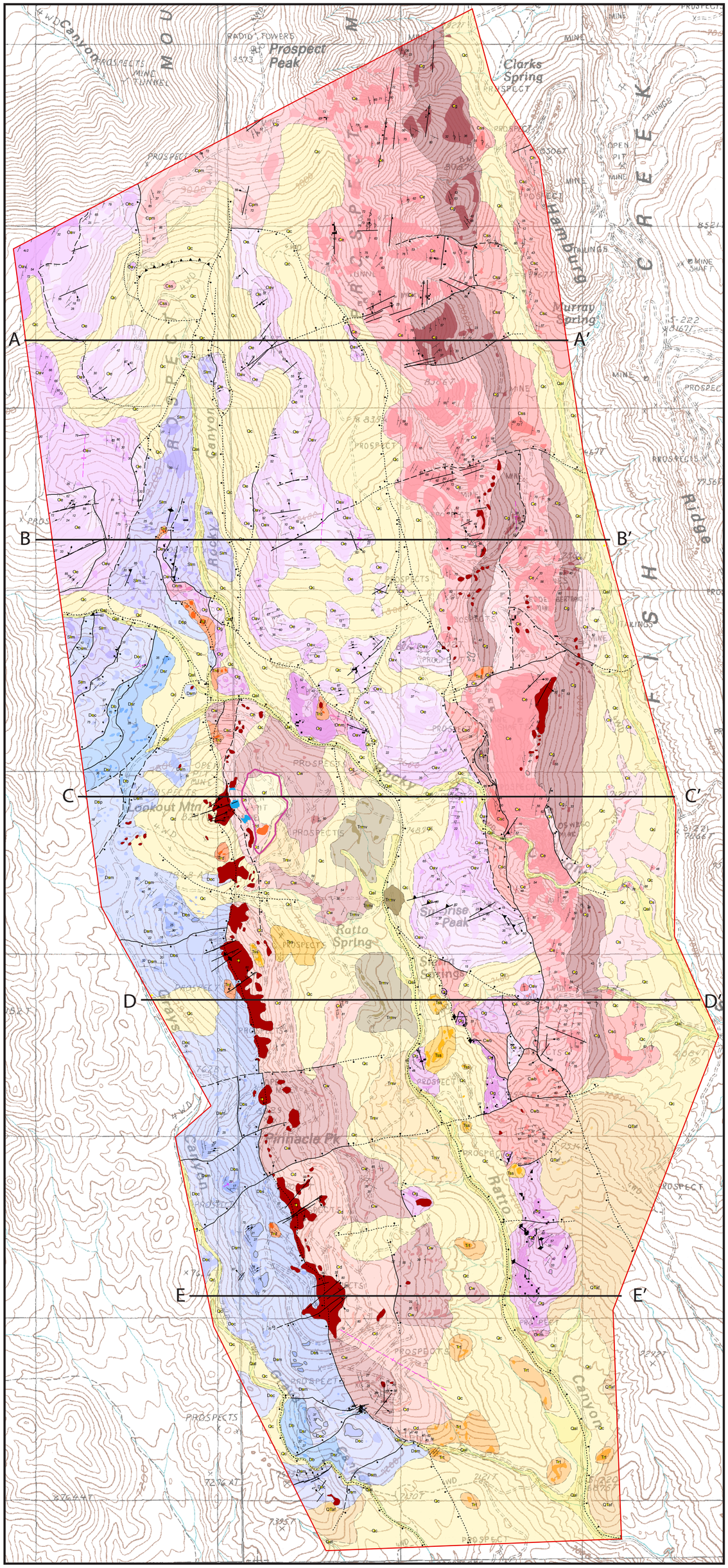

Correlation of Map Units

Quaternary

- Qf – artificial fill
- Qal - alluvium
- Qc - colluvium
- QTaf – alluvial fan

Tertiary

- Trmv – Richmond Mountain dacite and andesite
- Tpr - Pinto Peak rhyolite
- Tss – Sierra Springs Tuff Member
- Trt - Pinto Basin Tuff Member
- Trd – rhyolite dike
- Trsv - Ratto Springs Rhyodacite

Devonian

- Dn - Nevada Formation
- Dbs - Bay State dolostone member
- Dsm - Sentinel Mountain dolostone member
- Doc - Oxyoke Canyon sandstone member
- Dbp - Beacon Peak dolomite

Silurian

- Slm - Lone Mountain dolomite
- Ohc - Hanson Creek Formation

Ordovician

- Oe - Eureka quartzite
- Op - Pogonip Group
- Oav: Antelope Valley Formation
- Onm - Ninemile Formation
- Og - Goodwin limestone
- Cw - Windfall Formation
- Cwb – Bullwhacker member
- Cwc – Catlin member

Cambrian

- Cd - Dunderberg shale member
- Ch - Hamburg dolomite
- Cs - Secret Canyon shale
- Csc - Clarks Spring member
- Css - Lower shale member
- Cg - Geddes limestone
- Ce - Eldorado Dolomite
- Cp - Pioche shale
- Cpm - Cpm - Prospect Mountain quartzite

Alteration

- Tjb - jasperoid
- Tcb - collapse breccia

Non Dn - Nevada Formation

- Dsr - Sadler Ranch member
- Db - Bartine (member of the McColley Canyon Formation)

Outline of Lookout Mountain pit

Scale 1:10,000

0.5 1 kilometer

0.5 1 mile

Adjoining 7.5′ Quadrangles Names

1	2	3	4
5	6	7	8
9	10	11	12

1 Hay Ranch
2 Devon Peak
3 Eureka
4 Diamond Peak
5 Combs Peak
6 Spring Valley Summit
7 Pinto Summit
8 Silverado Mountain
9 West of Bellvue Peak
10 Bellvue Peak
11 Pinto Summit SW
12 Black Point

Map Location

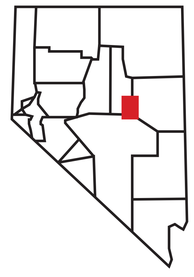

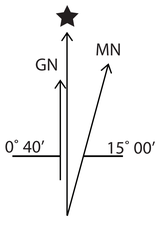

UTN GRID AND
1990 MAGNETIC NORTH
DECLINATION AT CENTER OF MAP AREA

Map Symbology

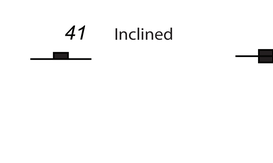

Contact: Solid where certain and location accurate, long-dashed where approximate, short-dashed where inferred, dotted where concealed.

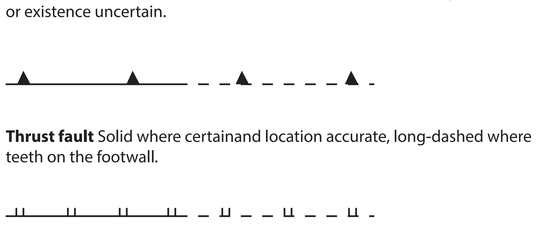

Normal fault Showing dip of fault and trend of striae on the fault surface (arrow); ball on downthrown side; solid where certain and location accurate, long-dashed where approximate, dotted where concealed, queried if identity or existence uncertain.

Thrust fault Solid where certainand location accurate, long-dashed where apporximate; teeth on the footwall.

Detachment fault Solid where certain and location accurate, long-dashed where approximate; pegs on the footwall.

Syncline Solid where certainand location accurate, long-dashed where approximate.

A A′

Line of cross-section

Strike and dip of bedding

41 Inclined Vertical

Strike and dip of breccia foliation

33 Inclined Vertical

Strike and dip of joints

41 Inclined Vertical

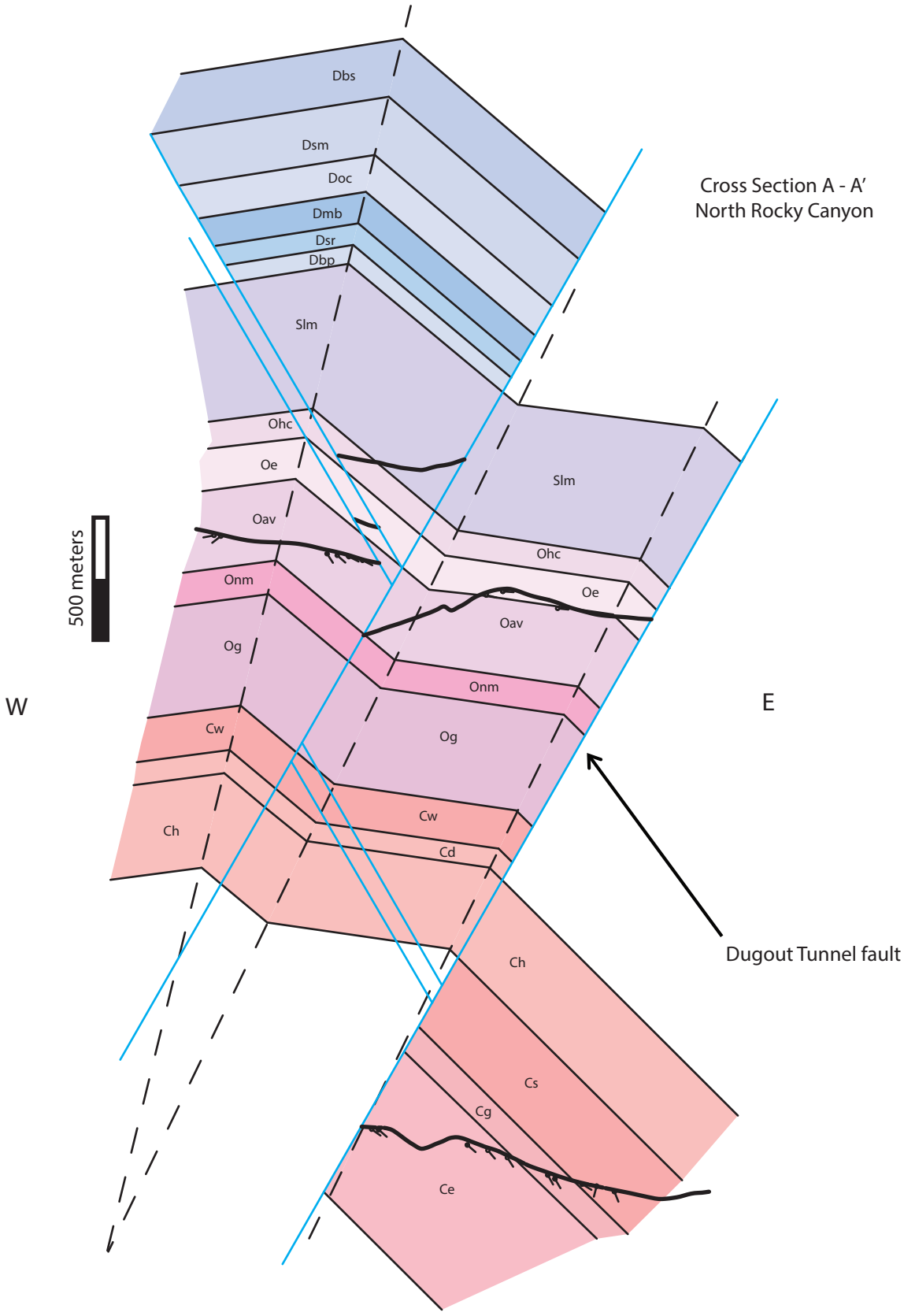
Cross Section A - A'
North Rocky Canyon
W
E
500 meters
Dugout Tunnel fault
Dbs
Dsm
Doc
Dmb
Dsr
Dbp
Slm
Ohc
Oe
Oav
Onm
Og
Cw
Ch
Cd
Cs
Cg
Ce

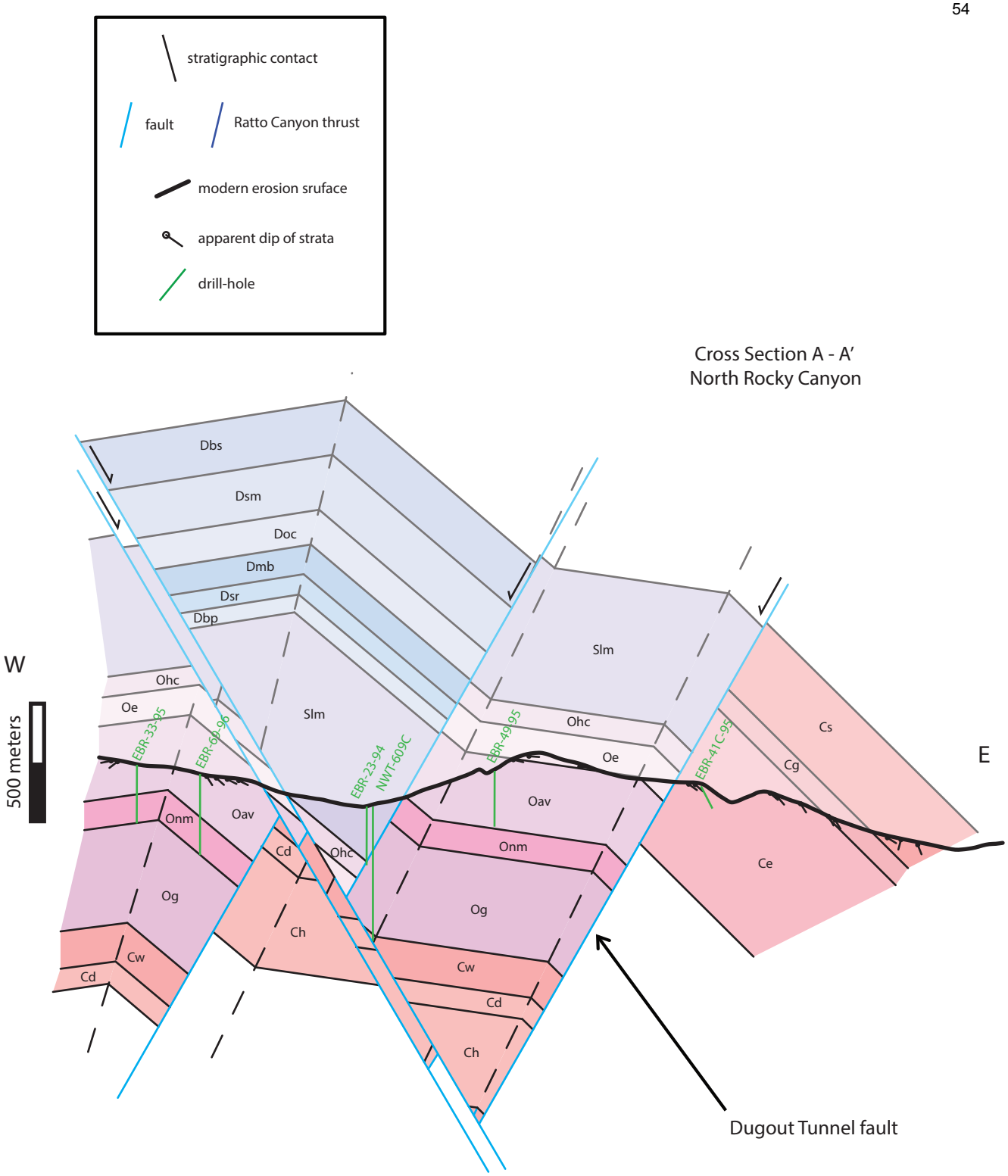
stratigraphic contact
fault
Ratto Canyon thrust
modern erosion sruface
apparent dip of strata
drill-hole
Cross Section A - A'
North Rocky Canyon
W
E
500 meters
Dbs
Dsm
Doc
Dmb
Dsr
Dbp
Slm
Ohc
Oe
Oav
Onm
Og
Cd
Ch
Cw
Cs
Cg
Ce
EBR-33-95
EBR-60-96
EBR-23-94
NWT-609C
EBR-49-95
EBR-41C-95
Dugout Tunnel fault

Cross Section B - B'
South Rocky Canyon

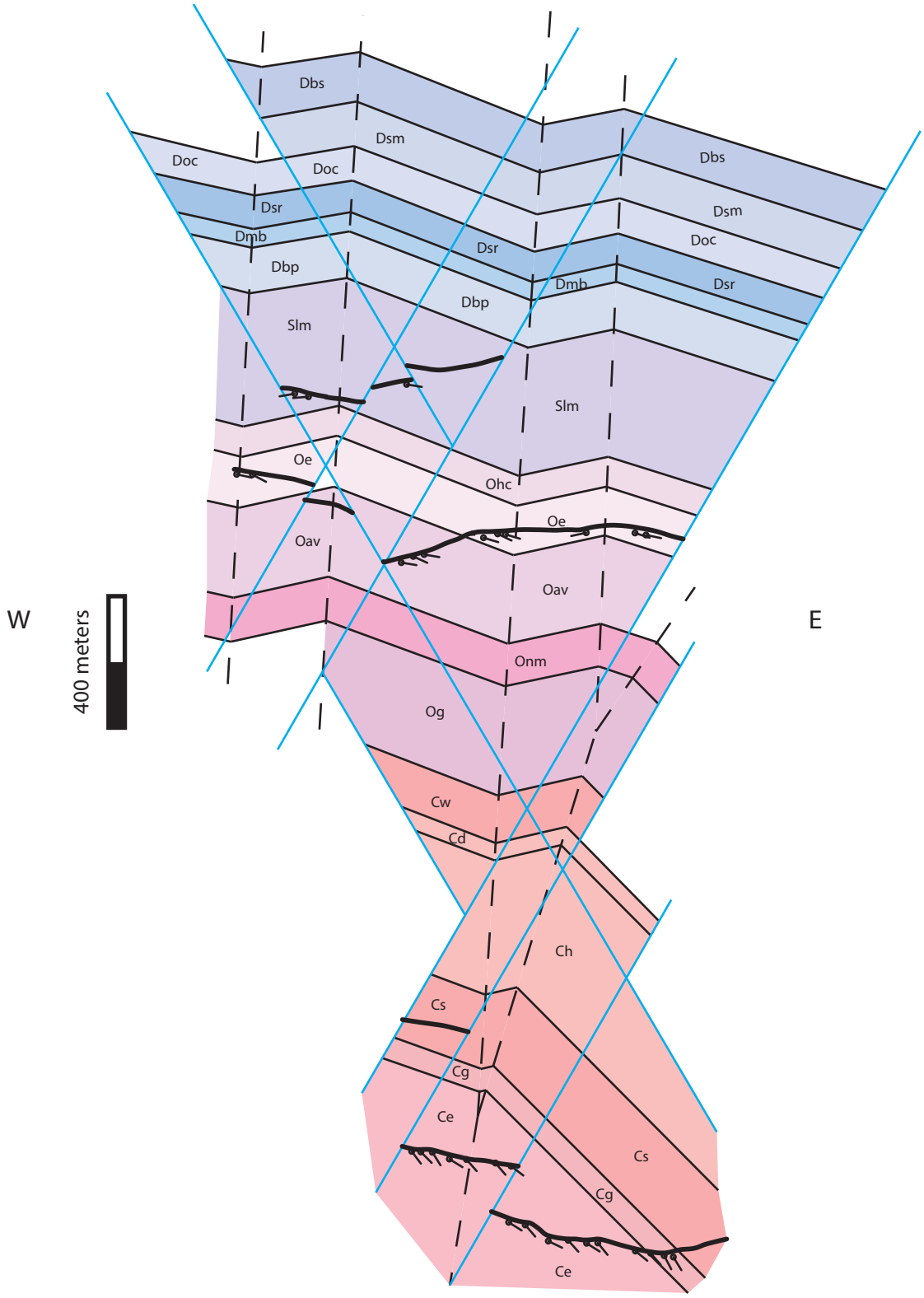

Cross Section B - B'
South Rocky Canyon

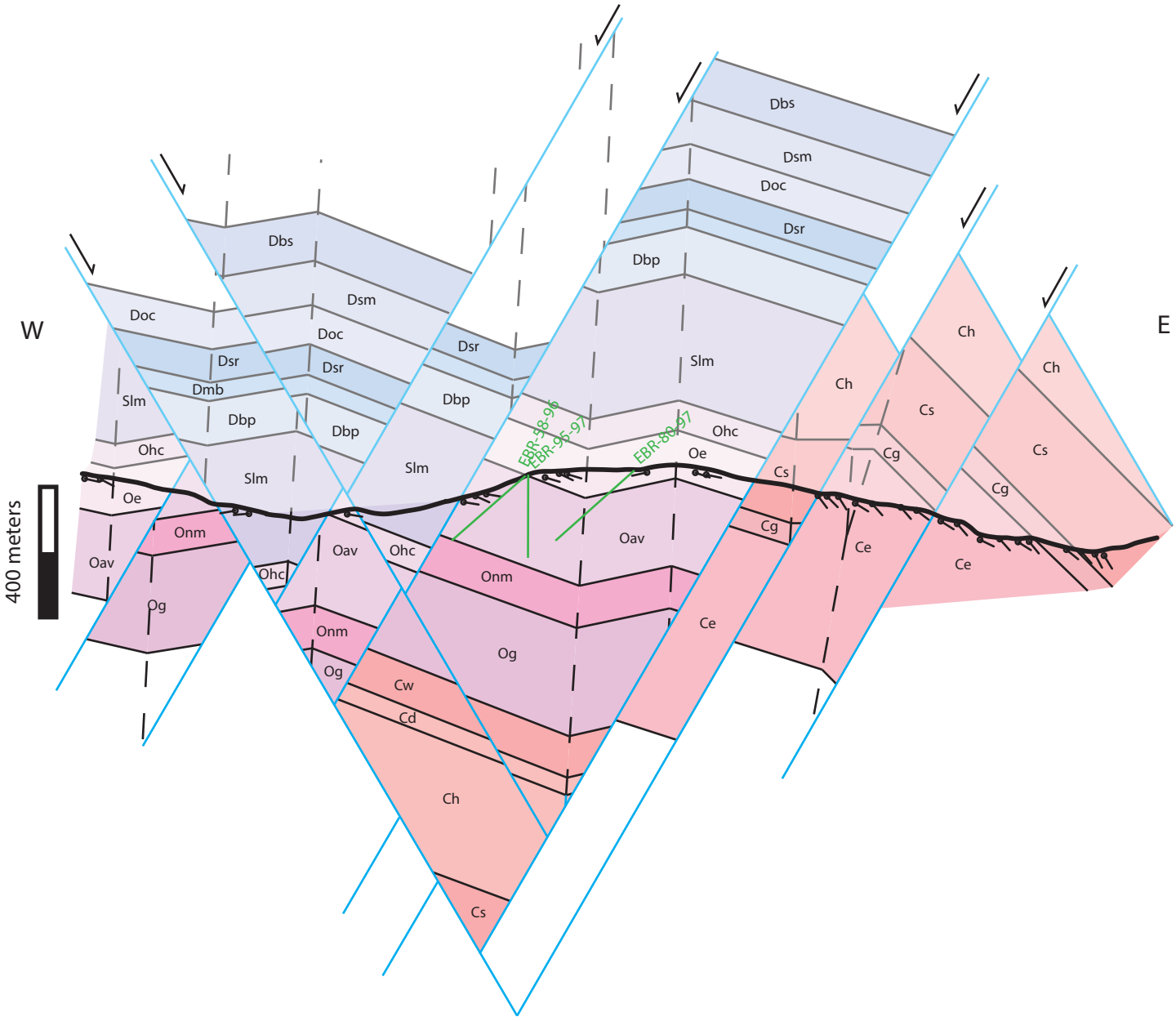

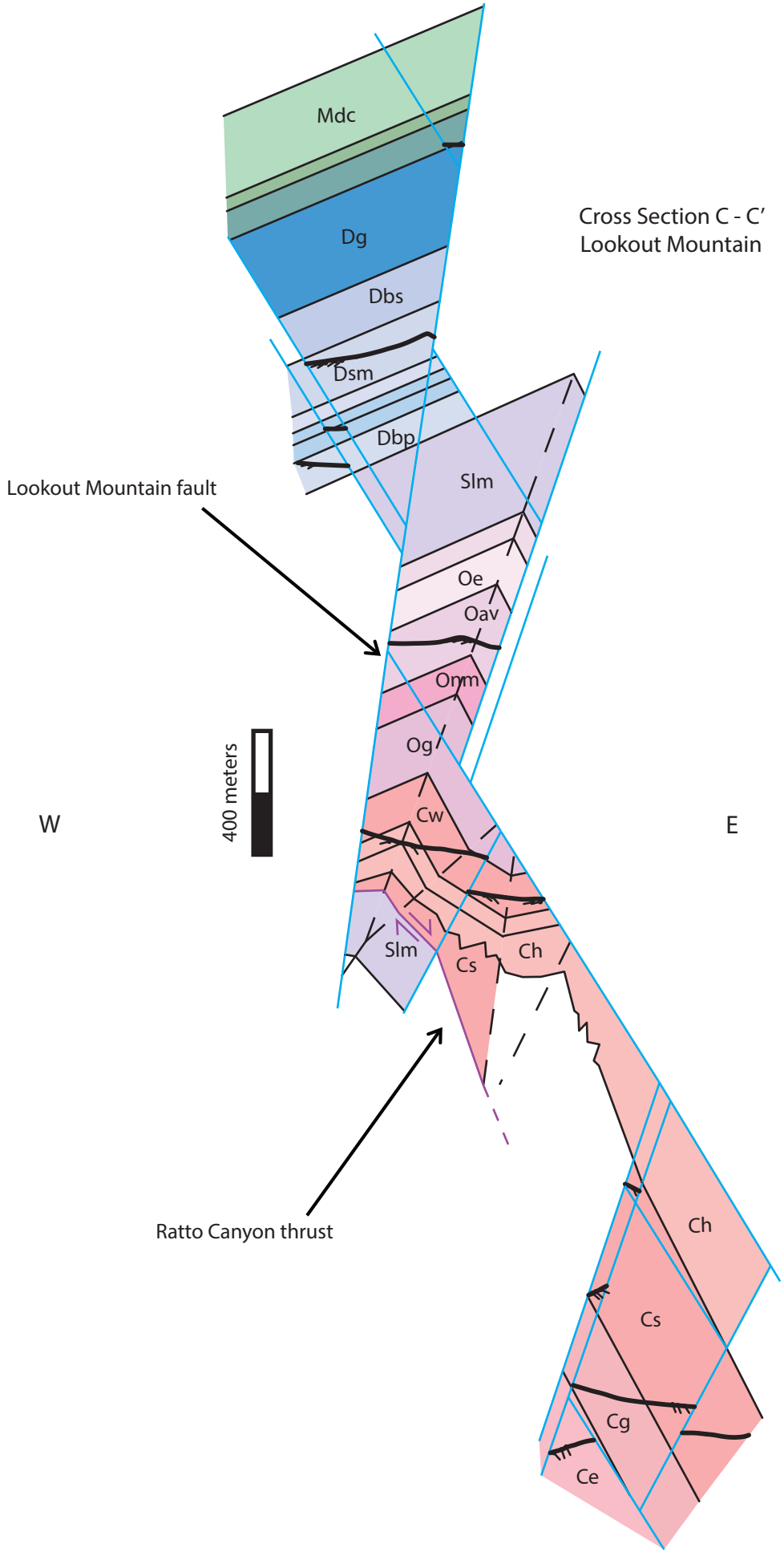
Cross Section C - C'
Lookout Mountain
Mdc
Dg
Dbs
Dsm
Dbp
Slm
Lookout Mountain fault
Oe
Oav
Onm
Og
400 meters
W
E
Cw
Slm
Cs
Ch
Ratto Canyon thrust
Ch
Cs
Cg
Ce

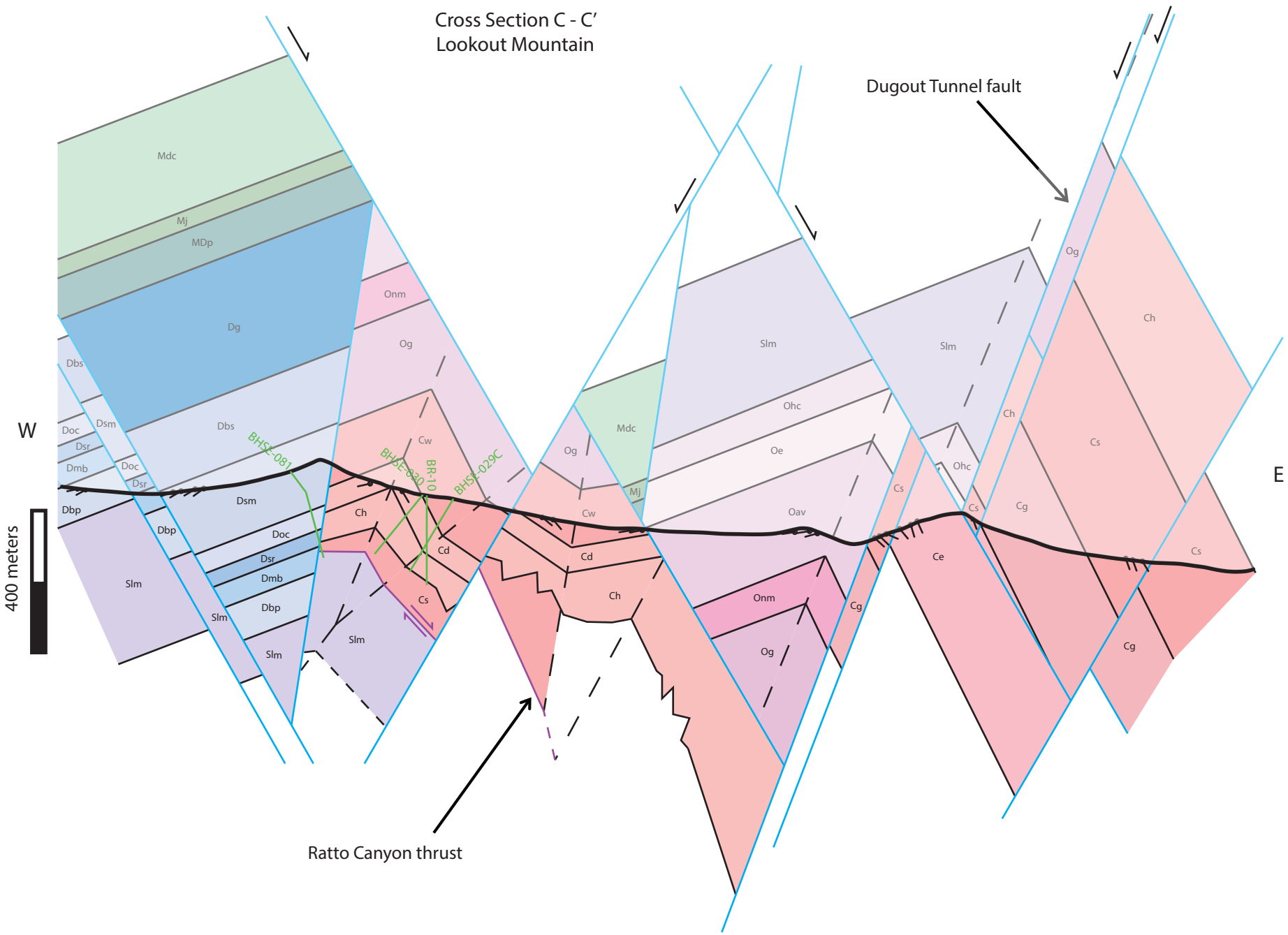

*Ch thins to the east, as it approaches on the Lookout Moutnain fault, due to volume loss due to dissolution

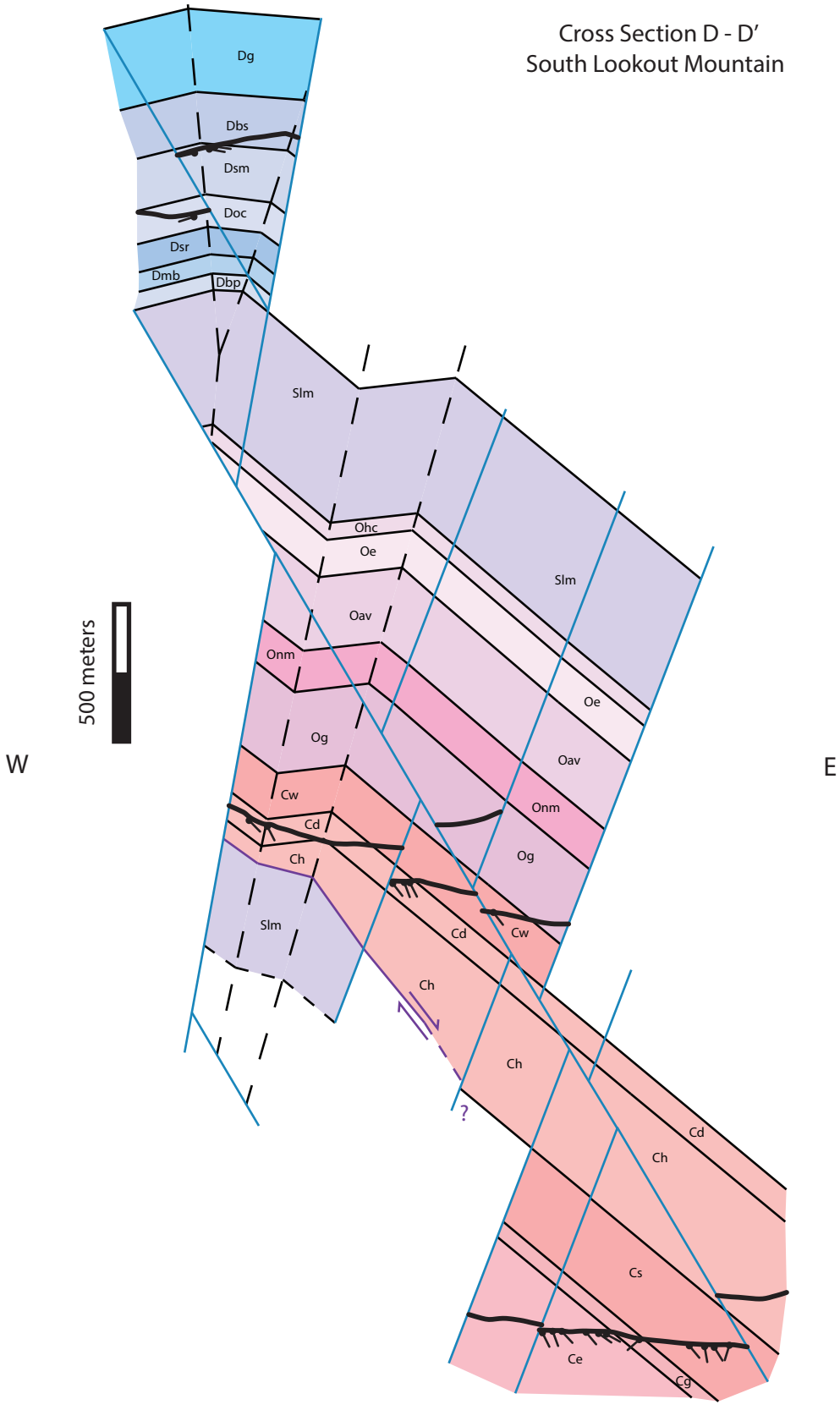
Cross Section D - D'
South Lookout Mountain
W
E
500 meters
Dg
Dbs
Dsm
Doc
Dsr
Dmb
Dbp
Slm
Ohc
Oe
Oav
Onm
Og
Cw
Cd
Ch
?
Cs
Ce
Cg

Cross Section D - D'
South Lookout Mountain

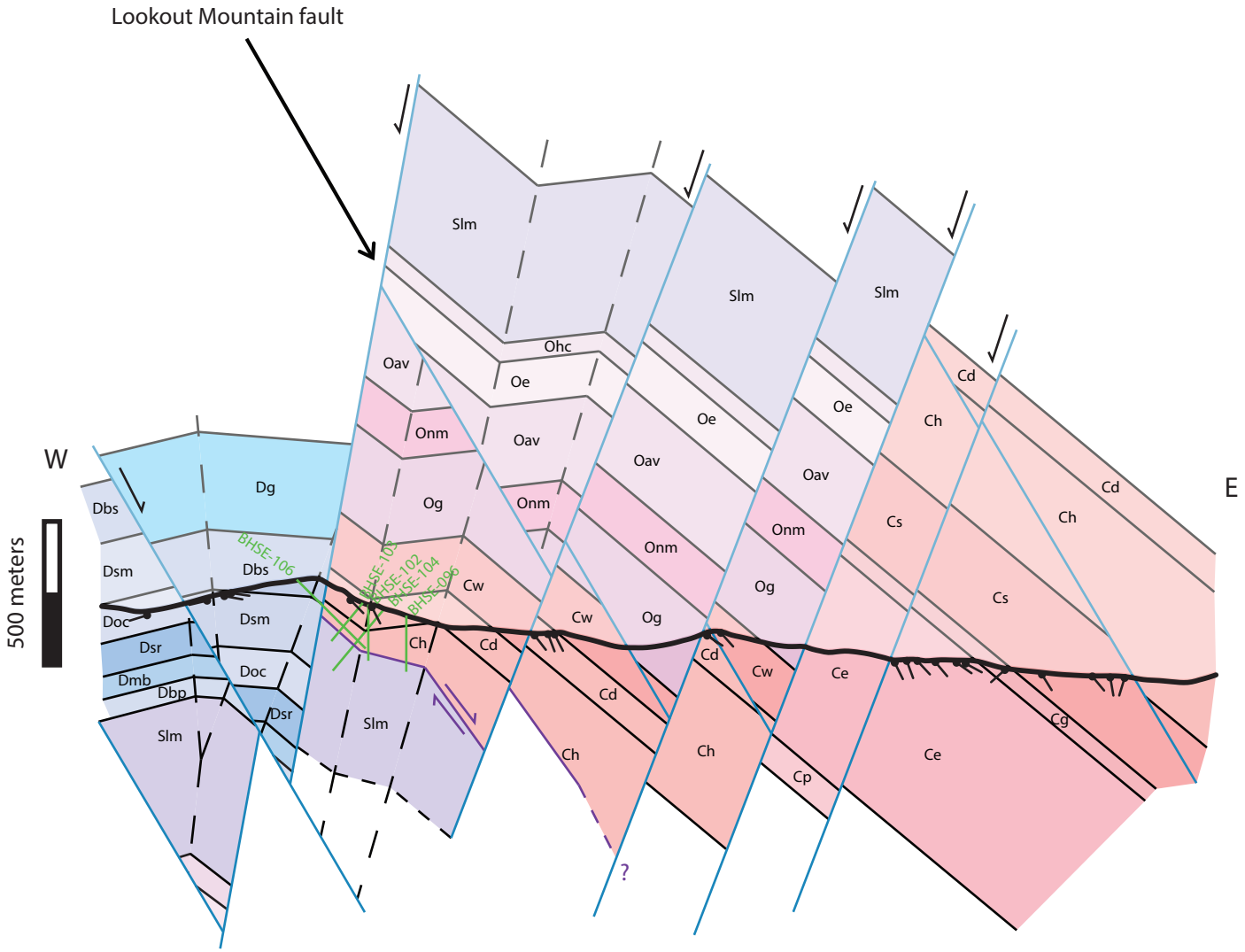

Cross Section E - E'
South Adit

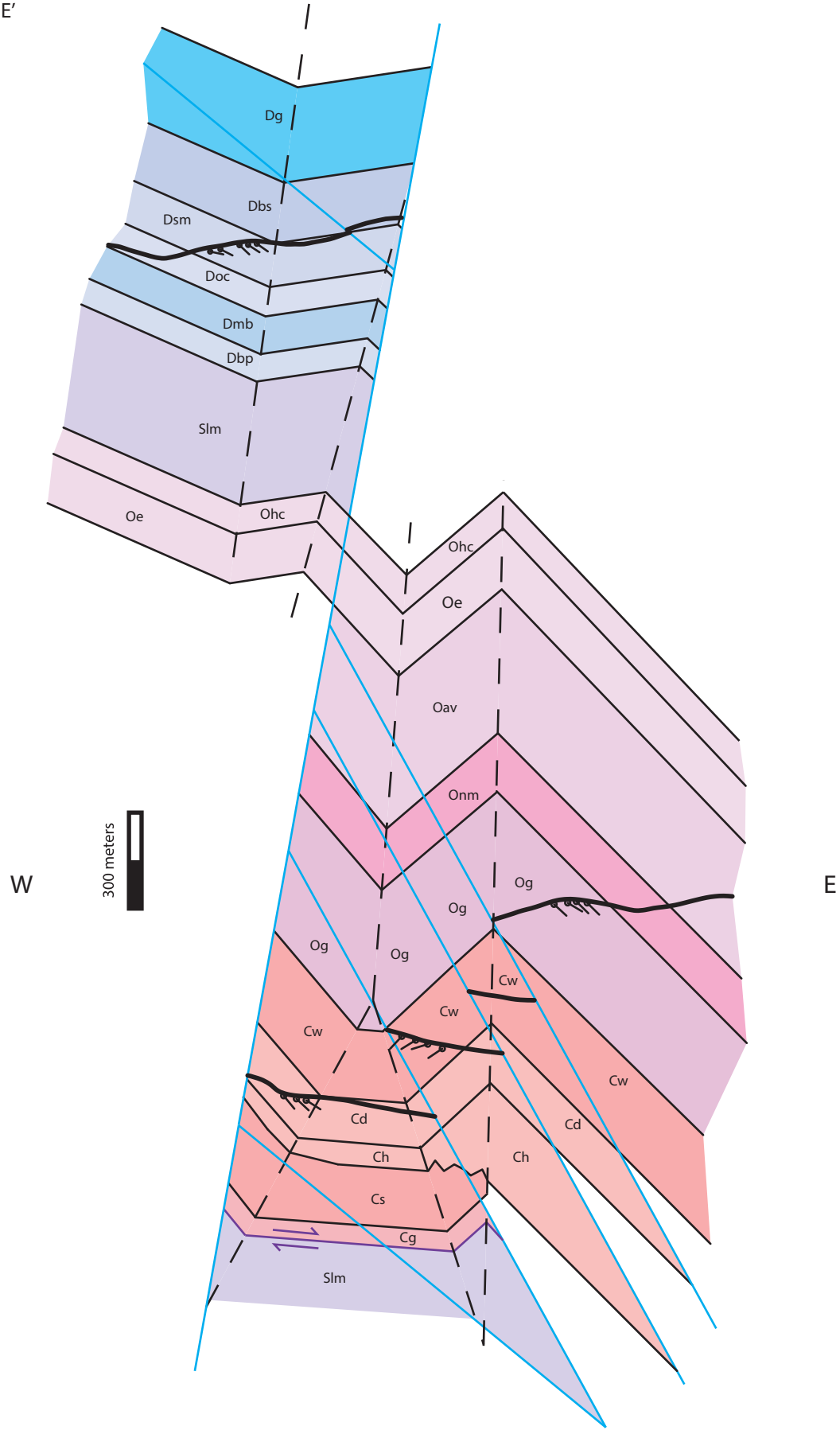

Cross Section E - E'
South Adit

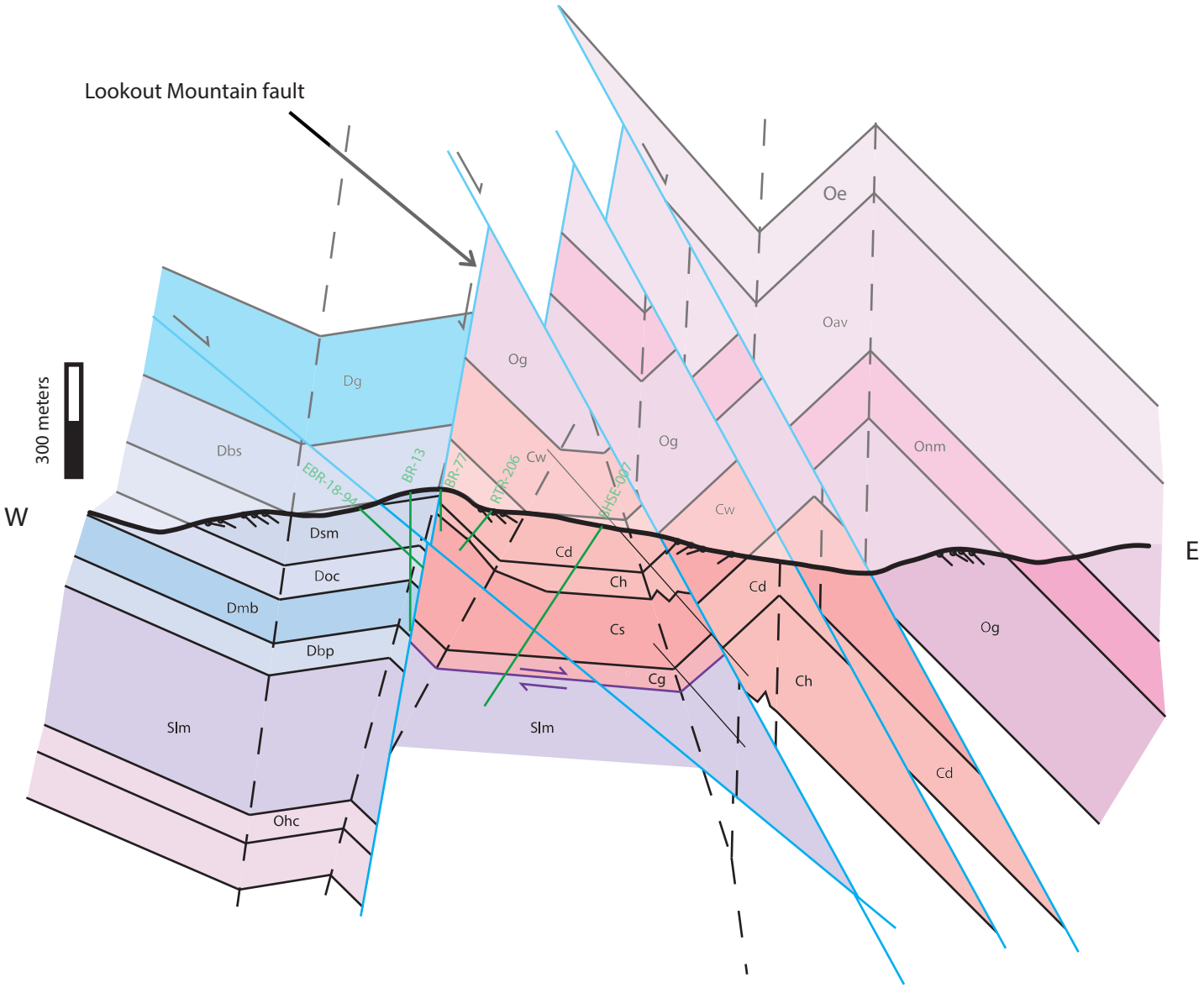

*Tertiary and Quaternary rock units omitted for simplicity